



## Workshop on Dynamics of Monitored Quantum Many-Body Systems | (SMR 3868)

21 Aug 2023 - 25 Aug 2023  
ICTP, Trieste, Italy

---

**P01 - AMINI ABCHUYEH Mohsen**

Structural properties of local integrals of motion across the many-body localization transition via a fast and efficient method for their construction

**P02 - ARCECI Luca**

Entanglement of Formation of Mixed Many-Body Quantum States via Tree Tensor Operators

**P03 - AZSES Daniel**

Identification of Symmetry-Protected Topological States on Noisy Quantum Computers

**P04 - BEHRENDIS Jan**

Surface codes, quantum circuits, and entanglement phases

**P05 - BRIGHI Pietro**

Directional transport in unbalanced Floquet East-West model

**P06 - CARISCH Christian**

Quantifying measurement-induced quantum-to-classical crossover using an open-system entanglement measure

**P07 - CHAHINE Karim**

Entanglement transition in monitored free fermions in 2D

**P08 - DOGGEN Vincent Hendrik Elmer**

Evolution of many-body systems under ancilla quantum measurements

**P09 - DOS PRAZERES Fernando Luis**

Multipartite Entanglement Structure and different Thermalization Regimes

**P10 - FUX Eugen Gerald**

Non-Stabilizerness in a Monitored Quantum Many-Body System

**P11 - GHORBAN ZADEH MOGHADDAM Ali**

Exponential shortcut to measurement-induced entanglement phase transitions

**P12 - GIUDICI Giuliano**

Temporal Entanglement and Trotter Transitions in unitary quantum circuits

**P13 - HOVHANNISYAN Vahan**

Computation of Microcanonical Entropy at Fixed Magnetization of the Long-Range Interacting System

**P14 - JOSHI Lata Kh**

Many-body quantum chaos with randomized measurements

**P15 - KALSI Tara**

Scaling Theory of Ergodic Scrambling

**P16 - KISHONY Gilad**

Simulated cooling of fermionic systems on bosonic quantum hardware

**P17 - KOGAN Eugene**

The Shocks and the Kinks in Josephson Transmission Lines

**P18 - LEUNG Chun Yin**

Theory of free fermion dynamics under partial post-selected monitoring

**P19 - LIEGEOIS Luc Christine Pierre-Emile Benjamin**

Tunable tachyon mass in the PT-broken massive Thirring model

**P20 - LUMIA Luca**

Dynamics of non-gaussianity under continuous measurements

**P21 - MEDINA GUERRA Edward**

On the noisy repeated interaction model

**P22 - MOCHIZUKI Ken**

Distinguishability and complexity in monitored dynamics of bosons

**P23 - MORRAL YEPES Raúl**

Entanglement Transitions in Unitary Circuit Games

**P24 - MUKHERJEE Aritro**

Dynamical Quantum State Reduction models via Spontaneous Unitarity Violation.

**P25 - OSHIMA Hisanori**

Measurement-induced criticality in a monitored circuit with U(1) charge conservation

**P26 - PASZKO Dawid**

Symmetry-protected topological order and cluster states in open quantum systems

**P27 - PAVIGLIANITI Alessio**

Multipartite Entanglement in the Measurement-Induced Phase Transition of the Quantum Ising Chain

**P28 - PUETZ Malte**

Stability of Nishimori cat states and non-equilibrium entanglement transitions

**P29 - RITU Ritu**

Topological phase transition in feedback control quantum systems

**P30 - ROY Sayan**

Resetting in the quantum dynamics of a particle in a long-ranged tight-binding model and subject to repeated measurements

**P31 - SANTINI Alessandro**

Full counting statistics as probe of measurement-induced transitions in the quantum Ising chain

**P32 - SIMM Jonathan Daniel**

Symmetry-enriched measurement-only quantum circuits on a Kitaev honeycomb lattice

**P33 - STARCHL Elias**

Entanglement dynamics of free fermions subjected to monitored loss and gain

**P34 - TSITSISHVILI Mikheil**

Diagrammatic method for many-body non-Markovian dynamics: memory effects and entanglement transitions

**P35 - ZERBA Caterina**

Measurement phase transitions in the no-click limit as quantum phase transitions of a non-hermitean vacuum

**P36 - ZHENG Chao**

Non-Hermitian Generalization of Rényi Entropy in Monitored Quantum Systems

# Structural properties of local integrals of motion across the many-body localization transition via a fast and efficient method for their construction

Safa Adami, Mohsen Amini <sup>\*</sup>, and Morteza Soltani

*Department of Physics, Faculty of Physics, University of Isfahan, Isfahan 81746-73441, Iran*



(Received 24 April 2022; revised 17 June 2022; accepted 1 August 2022; published 9 August 2022)

Many-body localization (MBL) is a novel prototype of ergodicity breaking due to the emergence of local integrals of motion (LIOMs) in a disordered interacting quantum system. To better understand the role played by the existence of such LIOMs, we explore and study some of their structural properties across the MBL transition. We first consider a one-dimensional XXZ spin chain in a disordered magnetic field and introduce and implement a nonperturbative, fast, and accurate method of constructing LIOMs. In contrast to already existing methods, our scheme allows obtaining LIOMs not only in the deep MBL phase but, rather, near the transition point too. Then, we take the matrix representation of LIOM operators as an adjacency matrix of a directed graph whose elements describe the connectivity of ordered eigenbasis in the Hilbert space. Our cluster-size analysis for this graph shows that the MBL transition coincides with a percolation transition in the Hilbert space. By performing finite-size scaling, we compare the critical disorder and correlation exponent  $\nu$  both in the presence and absence of interactions. Finally, we also discuss how the distribution of diagonal elements of LIOM operators in a typical cluster signals the transition.

DOI: [10.1103/PhysRevB.106.054202](https://doi.org/10.1103/PhysRevB.106.054202)

## I. INTRODUCTION

Currently, there is great scientific interest to gain deeper insight into the localization phenomena in many-body quantum systems. By now, it has been found that, in one dimension, an isolated interacting system of fermions that is subject to quenched disorder can undergo a phase transition from a thermal regime where transport is diffusive or subdiffusive [1–6] to the many-body localization (MBL) phase where the transport coefficients are exponentially small in the system size [7–10] and memory of the initial state is retained to arbitrarily long times [11].

It is thought that the MBL phase of such systems can be described in terms of emergent local integrals of motion (LIOMs) which form a complete set of quasilocal conserved quantities [12–14]. In the absence of interaction, such a system exhibits Anderson localization [15] for an arbitrarily small amount of disorder. The corresponding single-particle wave functions are exponentially localized in real space over a characteristic length scale which is called localization length. In this case, a complete set of LIOMs can be identified by the occupancies of these single-particle orbitals [12]. Upon turning the interaction on, multiparticle resonances start to proliferate and, hence, stronger disorder is needed to keep the system localized [7]. However, if the disorder strength is sufficiently larger than the interaction strength, the system remains in the MBL phase and LIOMs can be understood as weakly dressed single-particle orbitals [12,16].

In general, the number of ways in which a set of LIOMs can be arranged is very large and, therefore, the calculation

of all LIOMs is a complicated task practically. It was first pointed out that a complete set of LIOMs for a finite-size system can be obtained via labeling the eigenstates of the system by their corresponding LIOM eigenvalues uniquely [13,14]. Then, it was suggested to construct LIOMs (which do not form a complete basis) by computing an infinite-time average of initially local operators [17,18]. In this regard, various approaches like using Monte Carlo stochastic method [19], exact diagonalization techniques [20–23], and tensor networks [24–27] have been developed.

Although the above-mentioned construction algorithms for LIOMs have made great progress, developing and implementing a simple method that allows constructing a complete set of LIOMs with the following properties simultaneously is of major interest. A method that (i) is nonperturbative and provides quasilocal LIOMs that commute strictly with the Hamiltonian, (ii) not essentially requires strong disorder intensity, and (iii) costs much less computationally but yet has enough accuracy. In particular, the second property makes it possible to move away from the deep MBL phase toward the transition point and study some aspects of the phase transition using LIOMs. This is an interesting issue because even in the ergodic phase it is possible to define integrals of motion that are not local quantities. By increasing the strength of the disorder, one arrives in the MBL phase in which the system fails to thermalize and constants of motion are localized. Therefore, it is the structural properties of the LIOMs that directly affect the thermalization of the system [28]. So, it is always interesting to characterize the MBL transition via the properties of the LIOMs across the transition. Thus, the main objective of the following paper is twofold. First, we present an efficient scheme for computing a complete set of LIOMs in a nonperturbative manner and, second, capture certain aspects of the MBL transition by

<sup>\*</sup>msn.amini@sci.ui.ac.ir

considering the resulting LIOM operators as an adjacency matrix of a graph that represents the connectivity of the eigenbasis in the Hilbert-space and undergoes a percolationlike transition.

In this paper, we describe and develop a fast method to construct a complete set of LIOMs explicitly for the random-field XXZ spin chain that can be used to study some structural properties of LIOMs near the MBL to ergodic transition. We perform our algorithm via arranging an optimized set of the eigenstates of the system in a quasilocal unitary operator which maps the physical spin operators onto effective spins operators. Such an ordered set of the eigenbasis can be obtained by assigning an integer index number to each eigenstate which determines its order in our desired set. We recognize this index number by locating the original basis vector of the Hilbert space on which that eigenstate has the largest absolute amplitude among all the eigenstates of the system. Then, in the next step, we consider the resulting LIOM operator as an adjacency matrix of a network whose elements indicate the connectivity of the eigenbasis in the Hilbert space. We illustrate that this network undergoes a percolationlike transition on crossing the transition from MBL into the ergodic phase. The percolation transition can be understood within the Hilbert-space cluster size analysis of the fragmentation of the network associated with LIOMs. Such a classical percolation analogy for the MBL transition was previously observed either by considering the Hamiltonian as a tight-binding model in Fock space [29,30] or by retaining only resonant contributions and mapping the quantum problem to rate equations [31]. However, in this paper, we underline the importance of such a transition in a network associated with LIOMs which is a key concept in MBL transition. We further provide an analysis of how local observables on the clusters of this network can quantitatively capture the ergodic to MBL transition.

The rest of the paper is organized as follows. In Sec. II, we describe our spin-1/2 model employed and introduce our algorithm to construct LIOM operators. Section III contains numerical results obtained by the implementation of our algorithm. We first represent the results concerning the locality of obtained LIOM operators. We then use the LIOM operators and show that the ergodic to MBL transition coincides with a percolation transition in a graph of eigenvectors in the Hilbert space whose structure is described by the matrix representation of LIOMs. To illustrate how the transition takes place, we perform cluster size analysis and apply finite-size scaling to compare the percolation threshold and correlation exponent  $\nu$  in the presence and absence of interaction. We further discuss how the distribution of local magnetization of clusters may signals the transition and, finally, concluding remarks are given in Sec. IV.

## II. MODEL AND APPROACH

### A. Model Hamiltonian

We consider a standard model of MBL which is a spin-1/2 chain of length  $L$  in a random magnetic field in the  $z$  direction and can be written as

$$H = \sum_{i=1}^{L-1} J \left( \sigma_i^+ \sigma_{i+1}^- + \sigma_i^- \sigma_{i+1}^+ + \frac{1}{2} \Delta \sigma_i^z \sigma_{i+1}^z \right) + h_i \sigma_i^z, \quad (1)$$

where  $\sigma_i^\pm = \sigma_i^x \pm i\sigma_i^y$  are the raising and lowering spin-1/2 operators and  $\sigma_i^{x,y,z}$  denote the Pauli operators acting on spin  $i$ . Here, we use open boundary conditions and fix the exchange interaction coupling at  $J = 1$ . The values  $h_i$  are, also, drawn independently from a random uniform distribution  $[-W, W]$  and the parameter  $\Delta$  determines the anisotropy of the model. This model is known to undergo a phase transition at a critical disorder strength  $W = W_c = 3.5 \pm 0.5$  from an ergodic phase to an MBL phase which depends on energy density [32,33]. In the current paper, we focus on the MBL side of the transition,  $W > W_c$ , in which the existence of LIOMs prevents thermalization. Using the Jordan-Wigner transformation [34], this model can be mapped to a model of spinless fermions and we are interested in two different cases when  $\Delta = 0$  and  $\Delta = 1$ , which corresponds to the noninteracting Anderson model and an interacting and disordered fermionic model, respectively.

### B. Approach

To begin, let us review the basic idea behind the LIOM scheme. We first consider a noninteracting system in which  $\Delta = 0$ . Upon diagonalization of the Hamiltonian in Eq. (1), one obtains a set of energy eigenvalues that uniquely identifies the system's eigenstates. In this system, which is equivalent to a single-particle Anderson model, eigenstates are exponentially localized around some localization center and their occupation numbers are mutually commuting, conserved quantities, and hence can form a complete set of LIOMs. These are the number operators,

$$n_\alpha = \sum_{ij} \psi_\alpha^*(i) \psi_\alpha(j) c_i^\dagger c_j, \quad (2)$$

in terms of which the Hamiltonian can be rewritten as

$$H = \sum_{\alpha} 2\varepsilon_{\alpha} n_{\alpha} - \sum_{\alpha} \varepsilon_{\alpha}, \quad (3)$$

where the last term on the right-hand side is the vacuum constant energy shift. It is now straightforward to define the corresponding LIOM operators in terms of the original spin operators via the Jordan-Wigner string operator as

$$\tau_{\alpha}^z = 2 \sum_{ij} \psi_{\alpha}^*(i) \psi_{\alpha}(j) \sigma_i^+ \left( \prod_{k=\min(i,j)}^{\max(i,j)} \sigma_k^z \right) \sigma_j^- - 1, \quad (4)$$

which allows us to write the Hamiltonian as

$$H = \sum_{\alpha} \varepsilon_{\alpha} \tau_{\alpha}^z. \quad (5)$$

Given the locality of the  $\tau_{\alpha}$ , one could as well associate an index  $i$  of the lattice to each index  $\alpha$ , for example, considering the maximum of  $|\psi_{\alpha}(i)|^2$ .

In the presence of interactions, however, the basic idea behind the LIOMs scheme is to find a unitary transformation  $U$  that defines a similar complete set of independent pseudospin-1/2 operators:

$$\tau_i^z = U \sigma_i^z U^\dagger. \quad (6)$$

With the above considerations, the following properties are fulfilled by the  $\tau_i^z$  operators [12]:

(i)  $\tau_i^z$ 's are quasilocal operators, in the sense that

$$||[\tau_i^z, \sigma_j^a]|| < ce^{-|i-j|/\xi}, \quad (7)$$

for  $a = +, -, z$ , and some  $\xi, c$ .

(ii)  $\tau_i^z$  are exactly conserved operators and commute with each other:  $[H, \tau_i^z] = 0$  and  $[\tau_i^z, \tau_j^z] = 0$ .

(iii)  $\tau_i^z$  have eigenvalues  $\pm 1$  ( $(\tau_i^z)^2 = 1$ ) and each subspace has exactly dimension  $2^{L-1}$ .

The unitary  $U$  is a composition of local unitary transformations as described by Refs. [35,36]. With the same unitary transformation, one can also define  $\tau_i^\pm$ , which completes the Pauli algebra. Once the operators  $\tau_i^z$  has been determined, one can use it to write the Hamiltonian  $H$  as a sum of local terms of these interacting LIOMs as

$$H = \sum_i \varepsilon_i \tau_i^z + \sum_{ij} J_{ij} \tau_i^z \tau_j^z + \sum_{ijk} J_{ijk} \tau_i^z \tau_j^z \tau_k^z + \dots, \quad (8)$$

where the couplings between clusters of pseudospins  $J_{i_1, \dots, i_a}$  are local in the sense that they decay exponentially as a function of any couple of indices.

It is obvious that each arbitrary arrangement of the eigenvectors of Hamiltonian  $H$  in the unitary matrix  $U$  of Eq. (6) results in a new set of  $\tau_i$  operators which satisfy the above-mentioned properties (ii) and (iii) by default. However, we are interested in finding a complete set of  $\tau_i$  operators that also fulfills the quasilocal requirement which is defined in Eq. (7). Therefore, our goal is to identify a specific arrangement of the eigenstates in  $U$  that best fulfill properties (i)–(iii) altogether.

For all choices of  $W$  and  $\Delta$ , total magnetization is a conserved quantity which implies the conservation of the  $z$  component of the total spin,  $[S^z, H] = 0$  with  $S_i^z = \sum_{i=1}^L S_i^z$ . Therefore, it defines a good quantum number and we can consider different magnetization sectors separately. Throughout the paper, we use the standard notation  $|n\rangle \equiv |S_1^z, S_2^z, \dots, S_L^z\rangle$  with  $S_i^z = \uparrow, \downarrow$  for the basis states in real space. In this notation,  $n$  in  $|n\rangle$  is a decimal integer can be obtained from the  $L$ -bit binary representation  $|n_1 n_2 \dots n_L\rangle$  as  $n = \sum_{i=1}^L n_i 2^{i-1}$ , where  $n_i = 0, 1$  stands for  $S_i^z = \downarrow, \uparrow$  respectively. Using these basis states, we consider an initial set of the basis vectors  $\{|n\rangle\}$  in such a way that the Hamiltonian  $H$  is block diagonalized and each block corresponds to a subspace with a fixed magnetization. Here we are interested to introduce an efficient way of ordering the LIOM basis states. We use the idea of Ref. [14], which considers a one-to-one mapping between initial basis states  $|n\rangle$  and the eigenstates of the system and develop our own scheme to introduce a systematic way of performing such a mapping process. Therefore, we will use the same labeling scheme in which each LIOM basis state can be shown by a binary spectrum as  $|\tilde{n}\rangle \equiv |\tau_1^z, \tau_2^z, \dots, \tau_L^z\rangle$  with effective pseudospin  $\tau_i^z = \tilde{\downarrow}, \tilde{\uparrow}$ . Again, it is convenient to obtain the corresponding integer  $\tilde{n}$  for each LIOM basis vector from its binary representation as before. In what follows, we introduce an optimal ordered set of basis states that makes the unitary operator

$$U = \sum_n |\tilde{n}\rangle \langle n| \quad (9)$$

and can be used in Eq. (6) to form a complete set of LIOMs with our desired properties (i)–(iii).

We begin to construct our own approach by considering the noninteracting case, ( $\Delta = 0$ ). In this case, as we already mentioned, LIOMs can be characterized by conserved occupations of single-particle eigenstates and, hence, only the first term on the right-hand side remains in Eq. (8). We start with the reference state  $|0\rangle$  with all spins down as the only possible state in its magnetization sector which is also an eigenstate of the system. Therefore, it has a similar representation on both the original and LIOM basis, i.e.,  $|\underbrace{\downarrow \downarrow \dots \downarrow}_L\rangle = |\underbrace{\downarrow \downarrow \dots \downarrow}_L\rangle$ .

By flipping one spin in  $|0\rangle$ , we get a new state with  $S_i^z = L/2 - 1$  and since we have  $L$  places for this spin, we have  $L$  states in this sector. These states, which are supposed to be ordered according to their binary code, form the original basis states spanning the single-particle block of the Hamiltonian  $H$ . After diagonalizing Hamiltonian  $H$ , we obtain a set of eigenstates  $|\psi_m\rangle$  which needs to be ordered. According to the quasilocal criterion of Eq. (7), we expect an ordered set in which each pseudospin operator  $\tau_i^z$  is mostly localized around a physical spin operator in real space. Therefore, we can order the obtained eigenstates by determining their maximum overlap with the original basis states. For instance, the first eigenstate is the one that has maximum overlap with the first original basis state. Thus, we need to find the maximum available overlap among the set  $\{|\langle \uparrow \underbrace{\downarrow \downarrow \dots \downarrow}_{L-1} |\psi_m\rangle|^2, m =$

$1, \dots, L\}$ . If the  $m_0$ th eigenstate is the one with maximum overlap with the first original basis state, it is the first basis state in pseudospin space, which means that  $|\uparrow \underbrace{\downarrow \downarrow \dots \downarrow}_{L-1}\rangle = |\psi_{m_0}\rangle$ . By

the same token, it is possible to determine the  $j$ th eigenstate of this sector by defining the following sequence of eigenstate overlaps for the remaining eigenstates:

$$\{\alpha_m^j = |\langle \downarrow \dots \underbrace{\uparrow}_{j\text{th}} \downarrow |\psi_m\rangle|^2, \\ m = 1, \dots, m_0 - 1, m_0 + 1, \dots, L\}, \quad (10)$$

and finding the eigenstate which maximizes the above overlap and labeling it with  $|\downarrow \dots \underbrace{\uparrow}_{j\text{th}} \downarrow\rangle$ .

We now proceed to the next sector which has  $L(L-1)/2$  basis states with two flipped spins which can be represented by the following notation:

$$|j_1, j_2\rangle = S_{j_1}^+ S_{j_2}^+ |0\rangle = |\downarrow \dots \underbrace{\uparrow}_{j_2\text{th}} \dots \underbrace{\uparrow}_{j_1\text{th}} \dots \downarrow\rangle. \quad (11)$$

The indexes  $j_1$  and  $j_2$  immediately determine the associated integer number  $n$  of this basis vector accordingly. Therefore, if we are looking for the  $\tilde{n}$ th eigenstate in our optimized set, we should find the one with maximum overlap with its corresponding basis vector. That is, finding the maximum value among the following set of overlaps:

$$\{|\langle j_1, j_2 | \psi_m \rangle|^2, m = 1, \dots, L(L-1)/2\}, \quad (12)$$

and label it as  $\tilde{n}$ . The same analysis can be performed in higher-excitation sectors to arrange the final ordered set of the eigenstates properly.

Besides its ease of use and implementation, the main advantage of the above-mentioned algorithm is that it can be generalized even for the case of an interacting system ( $\Delta \neq 0$ ). At the same time, it provides an opportunity to consider the whole Hamiltonian in the full Hilbert-space of the system simultaneously. This is because each eigenstate has only nonzero amplitudes on the basis states of its own sector and hence, in our scheme there is a one-to-one mapping between initial basis states and their corresponding eigenstates of the same sector which prevents sector mixing. Consequently, if the initial basis states are chosen in such a way that the Hamiltonian is block diagonal, the resulting unitary matrix  $U$  of the eigenstates obtained after performing our ordering procedure is also block-diagonal. In the remainder of this subsection, we elaborate on the implementation of the algorithm which allows ordering a generic set of energy eigenstates of the system in such a way that the resulting LIOMs satisfy our desired properties (i)–(iii).

Suppose that we have an initial set of the basis vectors  $|n\rangle$  in which our Hamiltonian matrix is block diagonal. We can diagonalize this Hamiltonian and obtain the set of energy eigenbasis which is an arbitrary (but fixed) arrangement of energy eigenbasis of the system. Our aim is to rearrange them by assigning a decimal integer that determines their index in our final optimum set. Doing so, we use the fact that each eigenstate of the system is a  $2^L$  component vector which can be expanded based on the Hilbert-space original basis vectors  $|n\rangle$  as  $|\psi_i\rangle = \sum_{n'=1}^{2^L} A_{n'}^i |n'\rangle$ . We can label a given eigenbasis  $|\psi_i\rangle$  by integer number  $n$  if this eigenstate has the largest absolute amplitude on  $|n\rangle$  among all the eigenstates of the system. This means that one needs only to find the index  $n$  in such a way that  $|A_n^i|^2$  is the largest value of the set  $\{|A_n^i|^2, i = 1, \dots, 2^L\}$ . In other words, if we consider matrix  $U$ , which initially contains the eigenbasis of the Hamiltonian in its columns with an arbitrary arrangement, to find the  $n$ th eigenstate in our desired order, we need just to look at the  $n$ th row of  $U$  and determine which column has the maximum absolute value in this row. This procedure is represented graphically in Fig. 1. The repeated execution of this procedure results in our optimal arrangement of the eigenstates which can optimally satisfy our desired conditions. The procedure outlined above is accurate in the sense that the resulting LIOMs are exactly conserved operators and it is fast because it requires less computational effort as compared to other schemes [22–24] that are based on exact diagonalization. The reason is that in our method, unlike in the above-mentioned schemes, we no longer need to evaluate the expectation values of physical spin operators ( $L$  operations) for each energy eigenstate to determine its order in our desired set of eigenstates in  $U$ . This will reduce the computational cost associated with rearranging all the eigenstates in  $U$  by a factor of ( $L \times$  the number of eigenstates) totally. Consequently, since the procedure outlined above does not essentially require the strong disorder limit and, on the other hand, is very simple and fast, and we can use it to obtain our optimum and complete set of LIOMs rapidly and study some structural properties of the system across the phase transition.

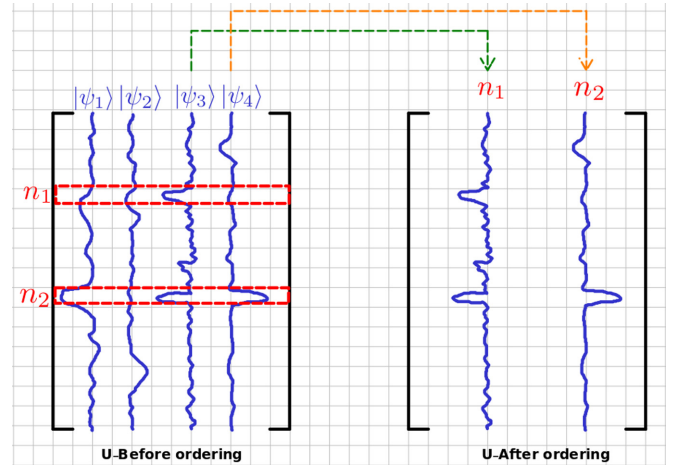


FIG. 1. Graphical representation of the procedure outlined in Sec. II B to arrange the eigenstates of the system in the unitary matrix  $U$  which is obtained after diagonalization. The left side shows the matrix of eigenvectors obtained via the exact diagonalization procedure in which usually the eigenstates are ordered according to their corresponding eigenvalues. The right side is the matrix of eigenstates after rearranging them using our algorithm.

### III. RESULTS

To examine our method, we have carried out numerical calculations based on the exact diagonalization technique. In what follows, we consider a spin chain with  $L$  spins and open boundary conditions. To gain a deeper understanding of the role of interaction in the MBL case, we consider our model in both interacting ( $\Delta = 1$ ) and noninteracting ( $\Delta = 0$ ) regimes, and depending on the system size  $L$ ,  $10^5$  to  $5 \times 10^3$  disorder realizations are employed to obtain the statistics.

#### A. Effective characterization of LIOM locality

In this section, we demonstrate the quasilocality of the resulting LIOM operators obtained by our algorithm. To this end, we use the two-point correlator between a LIOM operator  $\tau_j^z$  and physical spin  $\sigma_k$  which is expected [17,18,23] to decay exponentially with distance  $|k - j|$  as

$$\langle \tau_j^z \sigma_k^z \rangle = \text{Tr}(\tau_j^z \sigma_k^z) \sim \exp(-|k - j|/\zeta), \quad (13)$$

when  $j$  and  $k$  are far apart in the MBL regime. In Eq. (13),  $\zeta$  defines a length scale over which the corresponding LIOM operators are localized. This length scale is related to the spatial correlation length of the eigenstate amplitudes on the Fock space [37,38] and expected to diverge at the critical point.

Figure 2(a) shows the behavior of the logarithm of two-point correlator  $\langle \tau_j^z \sigma_k^z \rangle$  versus  $|j - k|$  for the LIOM operator which is located near the center of chain in the presence of interaction,  $\Delta = 1$ . It is obvious that in the deep localized regime ( $W \geq 5$ ), the LIOM operators  $\tau_j^z$  are strongly localized, and the  $\langle \tau_j^z \sigma_k^z \rangle$  profile is mostly localized near the origin  $j$  with a fast decaying function to the neighborhood. This is in contrast to the delocalized regime ( $W \leq 2.5$ ) in which such a fast decaying part is obviously absent. Furthermore, there is a clear size dependency, especially near the origin

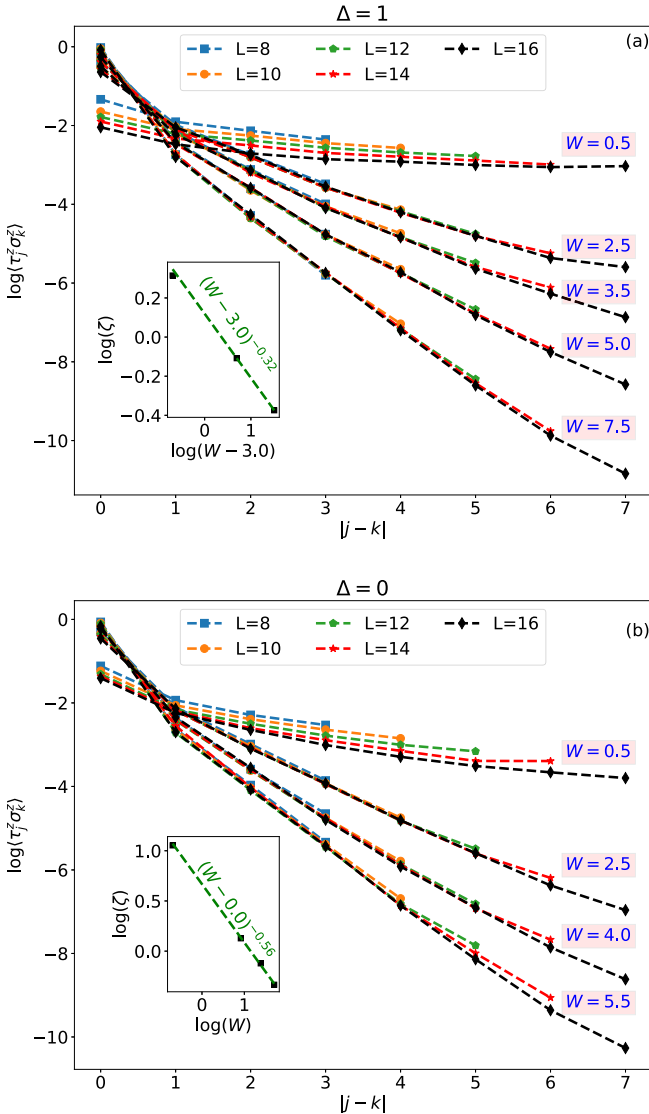


FIG. 2. Decay of two-point correlator  $[\log(\langle \tau_j^z \sigma_k^z \rangle)]$  for the LIOM operators localized near the chain center versus  $|j - k|$  for different system sizes  $L = 8 - 16$  and disorder intensities in both (a) interacting ( $\Delta = 1$ ) and (b) noninteracting ( $\Delta = 0$ ) regimes. Insets show the divergence of length scale  $\zeta$  as a function of  $(W - W_c)$  in the presence and absence of interaction, respectively

which is the characteristic feature of ergodic regime. To make a comparison with noninteracting system ( $\Delta = 0$ ), we have shown the behavior of the  $\langle \tau_j^z \sigma_k^z \rangle$  profile for this regime in Fig. 2(b). In this case ( $\Delta = 0$ ), even for very small disorder strength  $W = 0.5$  the faster decaying behavior as well as weaker size dependency can be observed in comparison to the MBL counterpart ( $\Delta = 1$ ).

It is also worth mentioning that the characteristic length scale  $\zeta$  can be extracted from the linear part of the  $\log(\langle \tau_j^z \sigma_k^z \rangle)$  versus  $|j - k|$  for the largest system size to observe its divergence near the transition point. The inset shows the power-law divergence of the  $\zeta$  as a function of  $(W - W_c)$  on approaching the transition point ( $W_c = 3.0$  and  $W_c = 0.0$  in the presence and absence of interaction, respectively) in the localized regime ( $W > W_c$ ).

Although the above comparison between the locality of LIOMs in both interacting and noninteracting systems is a piece of qualitative evidence for their difference in the sense of critical disorder needed for localization transition, we will elaborate on this more quantitatively in the coming sections and discuss the critical disorder  $W_c$  on which the transition takes place in detail.

## B. Percolation transition in connected clusters associated with LIOMs in the Hilbert space

In this section, we introduce a classical percolation problem associated with clusters of LIOMs in the Hilbert space. Indeed, LIOMs are dressed versions of spin operators as given by Eq. (6) and can be viewed as a matrix with elements  $(\tau_i^z)_{mn}$  ( $m$  and  $n$  refer to the row index and column index of this matrix, respectively) in the basis of product states in the  $S_z$  basis. Our idea is to interpret this matrix as an adjacency matrix representation of a finite directed graph in which the off-diagonal matrix elements of a given LIOM operator express whether two nodes (basis) are adjacent or not. According to the above discussion, we can write the adjacency matrix like the following:

$$C_{mn} = \begin{cases} 1, & \text{if } |(\tau_i^z)_{mn}| > \eta_c \\ 0, & \text{otherwise.} \end{cases} \quad (14)$$

Here,  $\eta_c$  is a connectivity threshold for deciding below which edge between a pair of basis states on the Hilbert-space graph will be removed or not. It is obvious that if  $\eta_c = 0$ , we always have a single connected cluster that contains all basis states of the Hilbert space. Therefore, we need to take a nonzero connectivity threshold,  $\eta_c > 0$ , for the rest of our analysis, which we will describe how to do in the following.

One detail should be described before discussing the estimation procedure. The point is to restrict our numerical calculations to the largest subspace with zero total spin, because the size of the Hilbert space grows exponentially and total magnetization is a conserved quantity in our system. This subspace contains  $N_H = \binom{L}{\frac{L}{2}}$  states (nodes). Thus, one naturally expects to have only a single connected cluster with size (number of nodes)  $N_H$  for a very weak disorder intensity, namely,  $0 < W \ll 1$ . This criterion will give us an upper bound for the parameter  $\eta_c$ . In our computation below, we take the maximum possible value for  $\eta_c$  according to its upper bound. Figure 3 shows a typical LIOM operator (represented as a matrix) and its adjacent Hilbert-space graph which is obtained with  $\eta_c = 0.05$  for a spin chain with  $L = 10$  spins for two random realizations of disorder with disorder strengths  $W = 2, 6$  in the MBL regime ( $\Delta = 1$ ).

### 1. Cluster-size analysis

In the theory of lattice percolation, the emergence of a spanning cluster at the percolation threshold which connects two opposite boundaries on the lattice is a measure of percolation transition [39]. It is obvious that such a definition doesn't really make sense for our considered network here. Therefore, in this subsection, we characterize the percolation transition by analyzing the size of the largest and second-largest connected cluster [40] associated with LIOMs in the

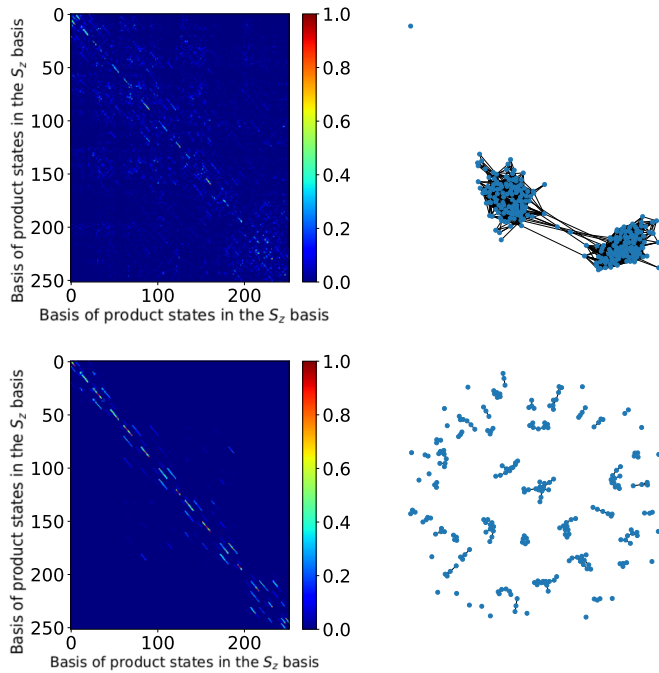


FIG. 3. The left side shows the graphical representation of matrix elements of a typical LIOM operator obtained using Eq. (6) and the ordered set of eigenvectors in unitary matrix  $U$ . The right side is the corresponding adjacent graph of the same LIOM operator in the basis of product states in the  $S_z$  basis for a spin chain with length  $L = 10$  spins for two different disorder intensities  $W = 2$  (upper panel) and  $W = 6$  (lower panel) in the MBL regime ( $\Delta = 1$ ).

Hilbert space. Starting from the low disorder limit,  $W \ll 1$ , we expect to have only a single connected cluster with size  $S_1 = N_H$  which contains all the nodes of Hilbert space. Due to the localization of eigenstates, one expects to observe a decrease in the largest cluster size by increasing the disorder intensity which means that it only contains a finite fraction of Hilbert-space nodes. In the percolation language, this is equivalent to the formation of smaller size clusters in the network.

We start to illustrate our percolation scenario by calculating the fraction of the largest cluster, defined as the relative size of the largest connected cluster with respect to the Hilbert-space dimension,  $S_1/N_H$ . Figure 4 shows how the mean largest cluster size which is averaged over different realizations of disorder decreases as a function of disorder intensity  $W$  for a spin chain of length  $L = 16$ . Additionally, we can also compute the average size of the second-largest cluster  $S_2$  to confirm the transition threshold. This is because, on finite systems, the size of the largest cluster grows by adding smaller clusters, and therefore it is possible to determine the vicinity of the transition point by locating the point where the second-largest cluster size reaches its maximum. The peak position coincides with the percolation threshold in the thermodynamic limit [40]. We observe that the normalized size of the second-largest cluster,  $S_2/S_2^{\max}$ , also peaks near the percolation transition. We have plotted the same quantities for both noninteracting and interacting regimes in Figs. 4(a) and 4(b), respectively, to make a comparison possible. It is obvious that the presence of interaction shifts the percolation

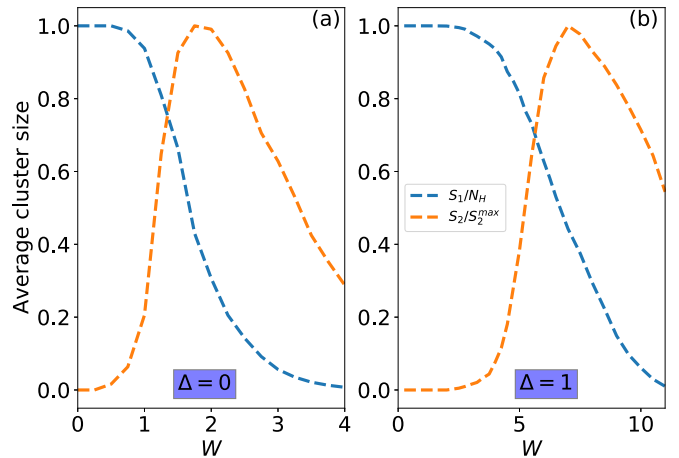


FIG. 4. Behavior of the average largest and second-largest cluster sizes versus disorder intensity  $W$  for a spin chain with  $L = 16$  spins in both (a) the noninteracting ( $\Delta = 0$ ) and (b) interacting ( $\Delta = 1$ ) regimes. It is obvious one needs a stronger disorder to reach the nonpercolating regime in the presence of interaction.

threshold  $W_c$  toward the stronger intensity of disorder, however, we leave the discussion of more accurate determination of such a percolation threshold for the sections that follow.

## 2. Universal feature and finite-size scaling analysis near the transition point

The more precise determination of the percolation threshold for the adjacent graph of the LIOMs can be obtained using scaling analysis. Following the arguments of Ref. [29], we first focus our attention on the scaling of the mean cluster size, and since the largest cluster is not essentially a typical one, we take the cluster  $C$  that contains the basis state of corresponding eigenstate  $|\psi_0\rangle$  with the closest energy to the mean value of the energy spectrum and compute the geometric average of its size over different realizations of disorder as

$$S_{\text{typ}} = \exp\left(\frac{1}{N_r} \sum_r \ln(s_r)\right). \quad (15)$$

Here,  $s_r$  is the number of nodes (eigenstates) in the cluster  $C$  for a given realization  $r$  of disorder and  $N_r$  is the number of disorder realizations. According to the finite-size scaling [39], the scaling of the normalized cluster sizes near the transition point can be stated as [29]

$$S_{\text{typ}}/N_H \sim f((W - W_c)L^{\frac{1}{\nu}}), \quad (16)$$

in which the exponent  $\nu$  is called the correlation length exponent. Therefore, by performing data collapse analysis, it is possible to obtain the percolation threshold  $W_c$  and critical exponent  $\nu$ . The results of such data collapse, yielding the critical exponent  $\nu(\Delta = 1) = 2.0$  and  $\nu(\Delta = 0) = 2.5$  in the presence and absence of interaction is shown in Figs. 5(a) and 5(b), respectively. We should emphasize that in the data collapse procedure in the noninteracting regime  $\Delta = 0$ , we constrained the critical point  $W_c = 0.0$  as a transition point of the corresponding XX model [41]. We note that the resulting exponent  $\nu$  satisfies the Harris-CCFS bound ( $\nu \geq \frac{2}{d}$ )

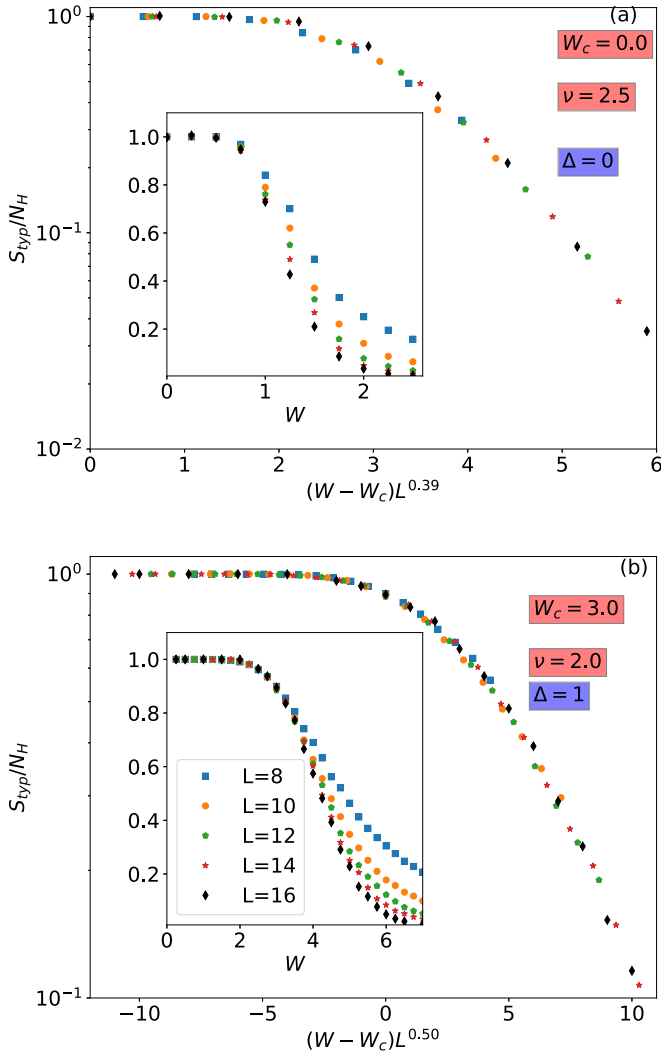


FIG. 5. The resulting data collapse of  $S_{\text{typ}}/N_H$  onto a scaling function of  $(W - W_c)L^{1/\nu}$  which is obtained for spin chains with different lengths ( $L = 8 - 16$ ) both in the (a) absence  $\Delta = 0$  and (b) presence  $\Delta = 1$  of interaction in the localized phase. The critical parameters  $W_c = 3.0, 0.0$ , and  $\nu = 2.0, 2.5$  is obtained for the case of MBL and Anderson transition, respectively. Insets show the corresponding raw data.

[42,43], confirmed for the ergodic to MBL transition recently [29,44,45].

In addition, the percolation threshold is quite different as  $W_c = 3.0$  and  $W_c = 0.0$  for the case of the interacting and noninteracting systems, respectively. It is worth mentioning that beyond the error of our analysis, the percolation threshold for the case of the interacting system coincides with the ergodic to MBL transition point  $W_c \approx 3.5$  [33], which shows that our system experiences a percolation transition in its corresponding LIOMs across the MBL transition.

Before ending this subsection, let us shed more light on the effect of changing the estimated parameter  $\eta_c$  in our clusterization mechanism. As we already discussed, we set the value of this parameter by the largest value of  $\eta_c$  for which the size of the largest cluster is exactly equal to the Hilbert-space dimension  $N_H$ . It is certainly possible to consider smaller

nonzero values for the connectivity threshold parameter (any value in  $(0, \eta_c]$ ). However, our investigations showed that the changing of  $\eta_c$  may change a bit the percolation threshold  $W_c$ , but the correlation length exponent  $\nu$  will not change.

### C. Distribution of local observables on the clusters

The last quantity which we are interested in is the distribution of the eigenstate expectation values of local observables which are shown to vary significantly across the MBL transition [46,47]. In doing so, let us consider cluster  $C$ , which contains the eigenstate  $|\psi_0\rangle$  with size  $s$ , as we discussed before, and define the following quantity for the cluster [29]:

$$m_l = \frac{1}{s} \sum'_n \langle n | \tau_l^z | n \rangle, \quad (17)$$

where  $\sum'$  denotes the restrictions imposed by considering only the eigenstates in  $C$  in summation. This is indeed the average local magnetization of the cluster and can be obtained by averaging only over the diagonal entries of the corresponding LIOM operator which belongs to the cluster  $C$ . We are interested in the distribution of this quantity which is averaged over different realizations of disorder.

Before going further, let us point out the meaning of the diagonal element of  $\tau_l^z$  using Eqs. (6) and (9),

$$\langle n | \tau_l^z | n \rangle = \sum_m (\sigma_l^z)_{mm} |\psi_m(n)|^2, \quad (18)$$

where  $\psi_m(n)$  represents the amplitude of the  $m$ th eigenstate on the  $n$ th basis state and  $(\sigma_l^z)_{mm}$  is the  $m$ th element of diagonal matrix  $\sigma_l^z$  with entries  $+1$  or  $-1$ . Now, the average local magnetization of cluster  $C$  defined in Eq. (17) can be expressed as

$$m_l = \frac{1}{s} \sum'_n \sum_m (\sigma_l^z)_{mm} |\psi_m(n)|^2. \quad (19)$$

Figure 6 shows the distribution of this quantity for the largest system size  $L = 16$  spins in both MBL and Anderson regimes. In the case of interacting regime  $\Delta = 1$  for weak disorder intensity  $W = 0.5$ , we have a single peak around zero. This is because in the ergodic phase, cluster  $C$  contains all the basis states of the Hilbert space and, hence,  $\sum'_n \rightarrow \sum_{n=1}^{N_H}$  and  $s = N_H$ . Therefore, it is convenient to perform the summation over  $n$  first and use the normalization condition of the eigenstates,  $\sum_n |\psi_m(n)|^2 = 1$ , which results in  $m_l = \text{Tr}(\sigma_l^z) = 0$ . This is the reason for observing a single peak at  $m_l = 0$  in the distribution function  $P(m_l)$  in Fig. 6 for weak disorder regime ( $W = 0.5$  and  $\Delta = 1$ ).

By increasing the disorder intensity  $W$ , since the size of cluster  $C$  starts to deviate (decreases) from the size of Hilbert space, some of the nodes (basis states) will be excluded from the summation over  $n$  in Eq. (19). Consequently, it is the eigenstate profile  $\psi_m(n)$  in Eq. (19) which plays a crucial role in characterizing the distribution function  $P(m_l)$  and one needs to know its exact form to describe the smooth part of  $P(m_l)$  in the intermediate regime  $W_c < W < \infty$ . For the case of very strong disorder limit ( $W \rightarrow \infty$ ), the probability of having only a single node in cluster  $C$  increases, which yields  $\psi_m(n) \sim \delta_{m,n}$  and  $s = 1$  and hence  $m_l = \pm 1$ . So one

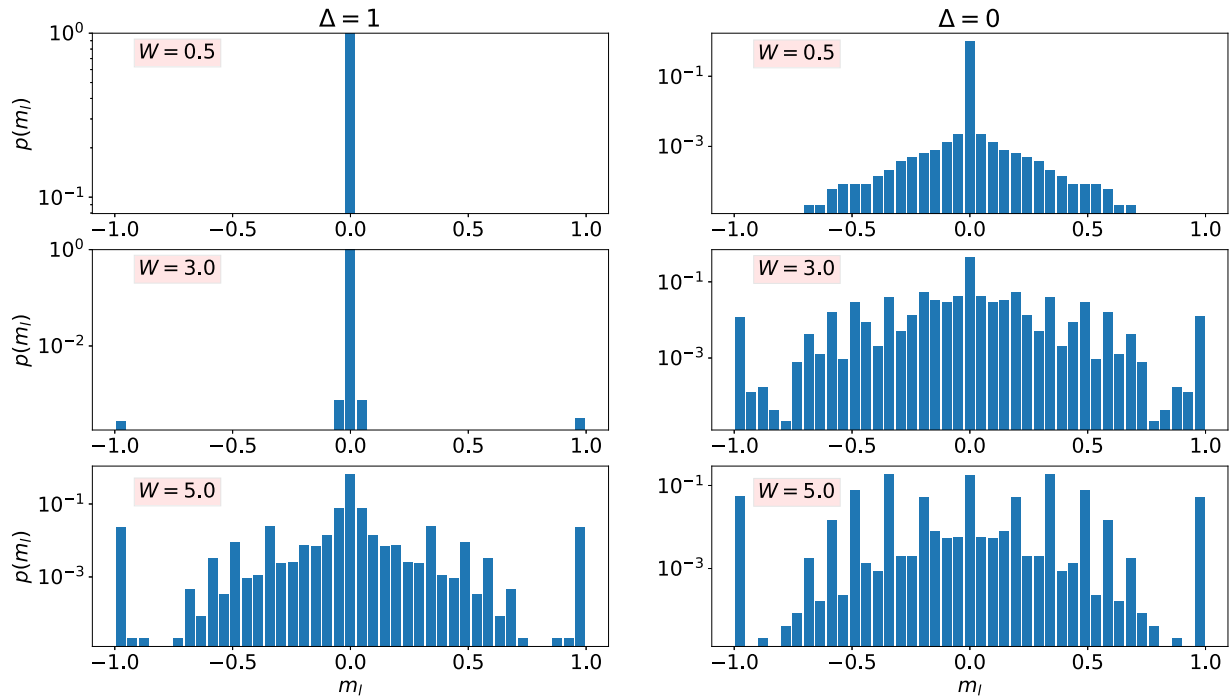


FIG. 6. Distribution function  $P(m_l)$  of the average local magnetization of cluster  $m_l$ , which is the average expectation values of LIOM operator  $\tau_i^z$  over the nodes of this cluster both for  $\Delta = 0$  and  $\Delta = 1$ .

naturally expects to observe two single peaks at  $m_l = \pm 1$  for the distribution function  $P(m_l)$  in this regime. The plots in Fig. 6 show that the existence of such single-node clusters is much more probable even for very small disorder intensities in the case of the noninteracting regime ( $\Delta = 0$ ).

#### IV. CONCLUDING REMARKS

We provided a fast and accurate method to efficiently obtain LIOMs for a disordered system that undergoes MBL transition. We showed that an optimized set of eigenvectors obtained by locating their maximum overlap with Hilbert-space basis can be used to obtain the desired set of LIOM operators. We showed that the resulting LIOMs experience a percolation transition in their graph representation in Hilbert space by increasing disorder intensity. We also compared the

critical disorder and critical exponent describing percolation transition for both interacting (MBL) and noninteracting (Anderson) regimes. Our analysis showed that there is a concrete connection between the ergodic to MBL transition and the structural properties of LIOMs in their graph representation on the Hilbert space.

#### ACKNOWLEDGMENTS

We are extremely grateful to A. Scardicchio for multiple illuminated discussions, insights, and guidance to improve our work. We acknowledge the CINECA award under the IS CRA initiative for the availability of high performance computing resources and support. M.A. acknowledges the support of the Abdus Salam (ICTP) associateship program.

- [1] K. Agarwal, S. Gopalakrishnan, M. Knap, M. Müller, and E. Demler, Anomalous Diffusion and Griffiths Effects Near the Many-Body Localization Transition, *Phys. Rev. Lett.* **114**, 160401 (2015).
- [2] I. V. Gornyi, A. D. Mirlin, and D. G. Polyakov, Interacting Electrons in Disordered Wires: Anderson Localization and Low- $T$  Transport, *Phys. Rev. Lett.* **95**, 206603 (2005).
- [3] D. M. Basko, I. L. Aleiner, and B. L. Altshuler, Metal-insulator transition in a weakly interacting many-electron system with localized single-particle states, *Ann. Phys.* **321**, 1126 (2006).
- [4] M. Žnidarič, A. Scardicchio, and V. K. Varma, Diffusive and Subdiffusive Spin Transport in the Ergodic Phase of a Many-Body Localizable System, *Phys. Rev. Lett.* **117**, 040601 (2016).

- [5] R. K. Panda, A. Scardicchio, M. Schulz, S. R. Taylor, M. Žnidarič, Can we study the many-body localisation transition, *Europhys. Lett.* **128**, 67003 (2020).
- [6] M. Schulz, S. R. Taylor, C. A. Hooley, A. Scardicchio, Energy transport in a disordered spin chain with broken  $U(1)$  symmetry: Diffusion, subdiffusion, and many-body localization, *Phys. Rev. B* **98**, 180201(R) (2018).
- [7] V. Oganesyan and D. A. Huse, Localization of interacting fermions at high temperature, *Phys. Rev. B* **75**, 155111 (2007).
- [8] M. Žnidarič, T. Prosen, and P. Prelovšek, Many-body localization in the Heisenberg XXZ magnet in a random field, *Phys. Rev. B* **77**, 064426 (2008).

- [9] J. H. Bardarson, F. Pollmann, and J. E. Moore, Unbounded Growth of Entanglement in Models of Many-Body Localization, *Phys. Rev. Lett.* **109**, 017202 (2012).
- [10] S. Gopalakrishnan, M. Müller, V. Khemani, M. Knap, E. Demler, and D. A. Huse, Low-frequency conductivity in many-body localized systems, *Phys. Rev. B* **92**, 104202 (2015).
- [11] A. De Luca and A. Scardicchio, Ergodicity breaking in a model showing many-body localization, *Europhys. Lett.* **101**, 37003 (2013).
- [12] V. Ros, M. Müller, and A. Scardicchio, Integrals of motion in the many-body localized phase, *Nucl. Phys. B* **891**, 420 (2015).
- [13] M. Serbyn, Z. Papić, and D. A. Abanin, Local Conservation Laws and the Structure of the Many-Body Localized States, *Phys. Rev. Lett.* **111**, 127201 (2013).
- [14] D. A. Huse, R. Nandkishore, and V. Oganesyan, Phenomenology of fully many-body-localized systems, *Phys. Rev. B* **90**, 174202 (2014).
- [15] P. W. Anderson, Absence of diffusion in certain random lattices, *Phys. Rev.* **109**, 1492 (1958).
- [16] J. Z. Imbrie, Diagonalization and Many-Body Localization for a Disordered Quantum Spin Chain, *Phys. Rev. Lett.* **117**, 027201 (2016).
- [17] A. Chandran, I. H. Kim, G. Vidal, and D. A. Abanin, Diagonalization and Many-Body Localization for a Disordered Quantum Spin Chain, *Phys. Rev. B* **91**, 085425 (2015).
- [18] S. D. Geraedts, R. N. Bhatt, and R. Nandkishore, Emergent local integrals of motion without a complete set of localized eigenstates, *Phys. Rev. B* **95**, 064204 (2017).
- [19] S. Inglis and L. Pollet, Accessing Many-Body Localized States through the Generalized Gibbs Ensemble, *Phys. Rev. Lett.* **117**, 120402 (2016).
- [20] L. Rademaker and M. Ortuño, Explicit Local Integrals of Motion for the Many-Body Localized State, *Phys. Rev. Lett.* **116**, 010404 (2016).
- [21] T. E. O'Brien, D. A. Abanin, G. Vidal, and Z. Papić, Explicit construction of local conserved operators in disordered many-body systems, *Phys. Rev. B* **94**, 144208 (2016).
- [22] M. Goihl, M. Gluza, C. Krumnow, and J. Eisert, Construction of exact constants of motion and effective models for many-body localized systems, *Phys. Rev. B* **97**, 134202 (2018).
- [23] P. Peng, Z. Li, H. Yan, K. X. Wei, and P. Cappellaro, Comparing many-body localization lengths via nonperturbative construction of local integrals of motion, *Phys. Rev. B* **100**, 214203 (2019).
- [24] A. Chandran, J. Carrasquilla, I. H. Kim, D. A. Abanin, and G. Vidal, Spectral tensor networks for many-body localization, *Phys. Rev. B* **92**, 024201 (2015).
- [25] D. Pekker and B. K. Clark, Encoding the structure of many-body localization with matrix product operators, *Phys. Rev. B* **95**, 035116 (2017).
- [26] F. Pollmann, V. Khemani, J. I. Cirac, and S. L. Sondhi, Efficient variational diagonalization of fully many-body localized Hamiltonians, *Phys. Rev. B* **94**, 041116 (2016).
- [27] T. B. Wahl, A. Pal, and S. H. Simon, Efficient Representation of Fully Many-Body Localized Systems using Tensor Networks, *Phys. Rev. X* **7**, 021018 (2017).
- [28] L. Rademaker, M. Ortuño, and A. M. Somoza, Many-body localization from the perspective of Integrals of Motion, *Ann. Phys.* **529**, 1600322 (2017).
- [29] S. Roy, J. T. Chalker, and D. E. Logan, Percolation in Fock space as a proxy for many-body localization, *Phys. Rev. B* **99**, 104206 (2019).
- [30] S. Roy, D. E. Logan, and J. T. Chalker, Exact solution of a percolation analog for the many-body localization transition, *Phys. Rev. B* **99**, 220201(R) (2019).
- [31] P. Prelovšek, M. Mierzejewski, J. Kršnik, and O. S. Barisic, Many-body localization as a percolation phenomenon, *Phys. Rev. B* **103**, 045139 (2021).
- [32] A. Pal and D. A. Huse, Many-body localization phase transition, *Phys. Rev. B* **82**, 174411 (2010).
- [33] D. J. Luitz, N. Laflorencie, and F. Alet, Many-body localization edge in the random-field Heisenberg chain, *Phys. Rev. B* **91**, 081103(R) (2015).
- [34] P. Jordan and E. Wigner, About the Pauli exclusion principle, *Z. Phys.* **47**, 631 (1928).
- [35] J. Z. Imbrie, On many-body localization for quantum spin chains, *J. Stat. Phys.* **163**, 998 (2016).
- [36] J. Z. Imbrie, V. Ros, and A. Scardicchio, Local integrals of motion in many-body localized systems, *Ann. Phys.* **529**, 1600278 (2017).
- [37] G. De Tomasi, I. M. Khaymovich, F. Pollmann, and S. Warzel, Rare thermal bubbles at the many-body localization transition from the Fock space point of view, *Phys. Rev. B* **104**, 024202 (2021).
- [38] S. Roy and D. E. Logan, Fock-space anatomy of eigenstates across the many-body localization transition, *Phys. Rev. B* **104**, 174201 (2021).
- [39] Percolation I, in *Fractals and Disordered Systems*, edited by A. Bunde and S. Havlin (Springer, Berlin, Heidelberg, 1991), pp. 51–96.
- [40] A. Margolina, H. J. Herrmann, and D. Stauffer, Size of largest and second largest cluster in random percolation, *Phys. Lett. A* **93**, 73 (1982).
- [41] T. Devakul, V. Khemani, F. Pollmann, D. A. Huse, and S. L. Sondhi, Obtaining highly excited eigenstates of the localized XX chain via DMRG-X, *Phil. Trans. R. Soc. A* **375**, 20160431 (2017).
- [42] A. B. Harris, Effect of random defects on the critical behaviour of Ising models, *J. Phys. C: Solid State Phys.* **7**, 1671 (1974).
- [43] J. T. Chayes, L. Chayes, D. S. Fisher, and T. Spencer, Finite-Size Scaling and Correlation Lengths for Disordered Systems, *Phys. Rev. Lett.* **57**, 2999 (1986).
- [44] A. Chandran, C. R. Laumann, and V. Oganesyan, Finite size scaling bounds on many-body localized phase transitions, [arXiv:1509.04285](https://arxiv.org/abs/1509.04285).
- [45] P. Sierant, M. Lewenstein, A. Scardicchio, and J. Zakrzewski, Stability of many-body localization in kicked Ising model, [arXiv:2203.15697](https://arxiv.org/abs/2203.15697).
- [46] C. L. Baldwin, C. R. Laumann, A. Pal, and A. Scardicchio, The many-body localized phase of the quantum random energy model, *Phys. Rev. B* **93**, 024202 (2016).
- [47] D. J. Luitz, Long tail distributions near the many-body localization transition, *Phys. Rev. B* **93**, 134201 (2016).

## Entanglement of formation of mixed many-body quantum states via Tree Tensor Operators

**L. Arceci<sup>1</sup>, P. Silvi<sup>2</sup>, and S. Montangero<sup>2</sup>**

<sup>1</sup> *Center for Quantum Physics, University of Innsbruck, 6020 Innsbruck, Austria*

<sup>2</sup> *Dipartimento di Fisica e Astronomia, Università di Padova, I-35131 Padova, Italy*

The Tree Tensor Operator (TTO) [1] is here introduced as a tensor network ansatz to efficiently represent certain classes of mixed many-body quantum states. The TTO guarantees positivity of the density matrix by construction and makes some quantities like purity and entropy easily accessible. Moreover, it is very suitable for the calculation of the Entanglement of Formation (EoF) [2], a notoriously hard, but very important problem for mixed many-body quantum states. We will show the application of the TTO to the calculation of the EoF for low-temperature thermal states of the 1D critical Ising model for up to 128 sites.

[1] Arceci L. et al, Phys. Rev. Lett. 128, 040501 (2022).

[2] Plenio, M., Virmani S., Quant. Inf. Comput. 7:1-51 (2007).

## Identification of Symmetry-Protected Topological States on Noisy Quantum Computers

D. Azses, R. Haenel, Y. Naveh, R. Raussendorf, E. Sela, and E. G. Dalla Torre

Identifying topological properties is a major challenge because, by definition, topological states do not have a local order parameter. While a generic solution to this challenge is not available yet, a broad class of topological states, namely, symmetry-protected topological (SPT) states, can be identified by distinctive degeneracies in their entanglement spectrum [1]. Here, we propose and realize two complementary protocols to probe these degeneracies based on, respectively, symmetry-resolved entanglement entropies and measurement-based computational algorithms [2]. The two protocols link quantum information processing to the classification of SPT phases of matter. They invoke the creation of a cluster state and are implemented on an IBM quantum computer. The experimental findings are compared to noisy simulations, allowing us to study the stability of topological states to perturbations and noise. [3]

- [1] D. Azses and E. Sela, Symmetry-resolved entanglement in symmetry-protected topological phases, *Phys. Rev. B* **102**, 235157 (2020).
- [2] R. Raussendorf, D. E. Browne, and H. J. Briegel, Measurement-based quantum computation on cluster states, *Phys. Rev. A* **68**, 022312 (2003).
- [3] D. Azses, R. Haenel, Y. Naveh, R. Raussendorf, E. Sela, and E. G. Dalla Torre, Identification of symmetry-protected topological states on noisy quantum computers, *Phys. Rev. Lett.* **125**, 120502 (2020).

## Surface codes, quantum circuits, and entanglement phases

**Jan Behrends<sup>1</sup>, Florian Venn<sup>2</sup>, and Benjamin Béri<sup>1,2</sup>**

<sup>1</sup>*T.C.M. Group, Cavendish Laboratory, University of Cambridge, J.J. Thomson Avenue, Cambridge, CB3 0HE, UK*

<sup>2</sup>*DAMTP, University of Cambridge, Wilberforce Road, Cambridge, CB3 0WA, UK*

Surface codes—leading candidates for quantum error correction (QEC)—and entanglement phases—a key notion for many-body quantum dynamics—have heretofore been unrelated. Here, we establish a link between the two. We map two-dimensional (2D) surface codes under a class of incoherent or coherent errors (bit flips or uniaxial rotations) to (1+1)D free-fermion quantum circuits via Ising models. We show that the error-correcting phase implies a topologically nontrivial area law for the circuit’s 1D long-time state  $|\Psi_\infty\rangle$ . Above the error threshold, we find a topologically trivial area law for incoherent errors and logarithmic entanglement in the coherent case. In establishing our results, we formulate 1D parent Hamiltonians for  $|\Psi_\infty\rangle$  via linking Ising models and 2D scattering networks, the latter displaying respective insulating and metallic phases and setting the 1D fermion gap and topology via their localization length and topological invariant. We expect our results to generalize to a duality between the error-correcting phase of  $(d+1)$ D topological codes and  $d$ -dimensional area laws; this can facilitate assessing code performance under various errors. The approach of combining Ising models, scattering networks, and parent Hamiltonians can be generalized to other fermionic circuits and may be of independent interest.

# Directional transport in unbalanced Floquet East-West model

P. Brighi<sup>1</sup>, M. Ljubotina<sup>2</sup>, and A. Nunnenkamp<sup>1</sup>

<sup>1</sup>*(Presenting author underlined) Faculty of Physics, University of Vienna,  
Boltzmannngasse 5, 1090, Vienna, Austria*

<sup>2</sup>*Institute of Science and Technology Austria (ISTA), am Campus 1, 3400,  
Klosterneuburg, Austria*

Kinetically constrained models have recently been object of intensive investigation, due to their relation with the topic of ergodicity breaking in terms of Hilbert space fragmentation and quantum many-body scars. In a few recent works [1, 2], the nature of transport in various kinetically constrained models was investigated, showing anomalous results ranging from strong subdiffusion to superdiffusion. Inspired by the rich landscape of transport properties of kinetically constrained models, in this work we introduce a binary driving protocol alternating two different kinetic constraints. The system is evolved for a first pulse under the particle-conserving East model Hamiltonian [3, 4], and subsequently a second pulse applies the analogous West Hamiltonian, where the action of the kinetic constraint is mirrored with respect to the East model. Our scheme is simple, yet the results are non-trivial due to the frustration in the dynamics induced by the competition of the two constraints. Using advanced numerical techniques, we investigate the system and explore its rich dynamical properties, showing state-dependent behavior ranging from localization to directional transport and eventually fast thermalization.

- [1] H. Singh, B. A. Ware, R. Vasseur and A. J. Friedman, Phys. Rev. Letters **127**, 230602 (2021).
- [2] M. Ljubotina, J. Y. Dossaules, Z. Papić and M. Serbyn, Phys. Rev. X **13**, 011033 (2023).
- [3] M. van Horssen, E. Levi and J. P. Garrahan, Phys. Rev. B **92**, 100305 (2015).
- [4] P. Brighi, M. Ljubotina and M. Serbyn, arXiv:2210.15607 (2022).

Measurement in Quantum Mechanics is among the most fundamental and debated processes in modern physics. In theory, it can be described by pure stochastic quantum trajectories, or continuous master equations for the mixed state. Whereas both descriptions lead to the same measurement statistics for linear observables, the quantum trajectory entanglement shows measurement-induced transitions (MITs) invisible to the steady-state density matrix. Moreover, there is no standard way to quantify the entanglement of mixed states. Recently, we have introduced the “configuration coherence”, a mixed-state entanglement measure for systems with a fixed conserved charge. Here, we employ the configuration coherence to demonstrate that entanglement in both the trajectories and master equation approaches reveal the MIT. Our finding suggests that the MIT is a manifestation of coherent-to-diffusive crossover in quantum random walks.

# Entanglement transition in monitored free fermions in 2D

K. Chahine<sup>1</sup>, M. buchhold<sup>1</sup>

<sup>1</sup>*Institut für Theoretische Physik, Universität zu Köln, D-50937 Cologne, Germany*

We examine the entanglement structure of a monitored fermionic system in  $d = 2$  dimensions. Both analytical considerations and numerical results point to a connection between this setting and the one of disorder-induced localization in  $d+1$  dimensions. This is studied both from the perspective of the measurement-induced entanglement transition and the observables typically considered in disorder-induced localization transitions, such as the inverse participation ratio (IPR). Our results suggest the presence of an entanglement transition from a phase with subextensive entanglement growth to an area-law regime. Furthermore, the IPR displays signature features of a metal to insulator transition.

## Evolution of many-body systems under ancilla quantum measurements

Elmer V. H. Doggen<sup>1,2</sup>, Yuval Gefen<sup>3</sup>, Igor V. Gornyi<sup>1,2,4</sup>,  
Alexander D. Mirlin<sup>1,2</sup> and Dmitry G. Polyakov<sup>1</sup>

<sup>1</sup>*Institute for Quantum Materials and Technologies, Karlsruhe Institute of Technology,  
76021 Karlsruhe, Germany*

<sup>2</sup>*Institut für Theorie der Kondensierten Materie, Karlsruhe Institute of Technology,  
76128 Karlsruhe, Germany*

<sup>3</sup> Department of Condensed Matter Physics, Weizmann Institute of Science, 7610001  
Rehovot, Israel

<sup>4</sup> Ioffe Institute, 194021 St. Petersburg, Russia

Measurement-induced phase transitions are the subject of intense current research, both from an experimental and a theoretical perspective. We explore the concept of implementing quantum measurements by coupling a many-body lattice system to an ancillary degree of freedom (implemented using two additional sites), on which projective measurements are performed. We analyze the effect of repeated (“stroboscopic”) measurements on the dynamical correlations of interacting hard-core bosons in a one-dimensional chain. An important distinctive ingredient of the protocol is the fact that the detector ancillas are not re-initialized after each measurement step. The detector thus maintains memory of the accumulated influence by the measured correlated system. Initially, we consider a model in which the ancilla is coupled to a single lattice site. This setup allows obtaining information about the system through Rabi oscillations in the ancillary degrees of freedom, modulated by the ancilla-system interaction. The statistics of quantum trajectories exhibits a “quantum-Zeno-valve effect” that occurs when the measurement becomes strong, with sharp branching between low and high entanglement. We proceed by extending numerical simulations to the case of two ancillas and, then, to measurements on all sites. With this realistic measurement apparatus, we find evidence of a disentangling-entangling measurement-induced transition as was previously observed in more abstract models. The dynamics features a broad distribution of the entanglement entropy.

[1] Elmer V. H. Doggen *et al.* arXiv:2303.07081.

[2] Elmer V. H. Doggen *et al.* Phys. Rev. Research **4**, 023146 (2022).

## Multipartite Entanglement Structure and different Thermalization Regimes

**Luis Fernando dos Prazeres<sup>1</sup>, Thiago Rodrigues de Oliveira<sup>1</sup>, and Fernando Iemini<sup>1</sup>**

<sup>1</sup>*Instituto de Física, Universidade Federal Fluminense, Niterói, Rio de Janeiro, Brazil*

Thermalization in closed quantum systems is still a discussed topic in physics. In classical mechanics, the mechanism behind thermalization is the chaoticity and ergodicity but for quantum systems, there is no trajectory in the classical sense, therefore to understand how thermalization emerges in quantum mechanics, physicists need to unfold different proprieties from nature to guarantee if a system is going to thermalize or not. One of the attempts to explain this phenomenon was given by Deutsch in [1] and Srednicki in [2] and they discussed that the eigenstates of the Hamiltonian can give thermal properties of some observables given that the expectations values of this observables in the energy eigenbasis do not vary too much for neighbor eigenstates. This idea is called the eigenstate thermalization hypothesis (ETH).

Moreover, the system of interest is not alone in the way of thermalizing. The pertinent question is: Given an initial condition for some Hamiltonian the expectation value of an observable  $\hat{A}$  would be thermal? In this work, we want to discuss how entanglement dynamics can unfold the peculiar thermal properties of the system. We study a Hamiltonian which shows two thermalization regimes known as weak and strong thermalization [3], the model studied was realized experimentally in [4], observing both. Strong thermalization occurs when the initial state evolves to the equilibrium value of the observable. Weak thermalization is the lack of equilibrium for some initial state, but its time average is thermal.

The results were obtained via exact diagonalization (ED) and we observed that entanglement dynamics from initial conditions which shows weak and strong thermalization has different entanglement structures, furthermore, the difficulty to reach the equilibrium value was also explained with the effective dimension for the initial state in the energy basis [5]. The connection between energy, effective dimension, and entanglement structure can be seen for each initial condition studied in [4] giving another point of view about why weak thermalization is observed.

[1] J. M. Deutsch Phys. Rev. A 43, 2046 (1991)

[2] Mark Srednicki Phys. Rev. E 50, 888 (1994)

[3] M. C. Bañuls, J. I. Cirac, and M. B. Hastings Phys. Rev. Lett. 106, 050405 (2011)

[4] Chen, Fusheng, et al, Phys. Rev. Lett., 127, 2, 020602, 6, 2021,

[5] T. R. de Oliveira, et al, New J. Phys. 20, 033032 (2018).

# Non–Stabilizerness in a Monitored Quantum Many–Body System

Gerald E. Fux<sup>1</sup> and Rosario Fazio<sup>1</sup>

<sup>1</sup>*The Abdus Salam International Center for Theoretical Physics (ICTP), Strada Costiera 11, I-34151 Trieste, Italy*

Entanglement phase transitions in monitored many–body open quantum systems have attracted a lot of attention in recent years. The robustness of the volume law phase against a finite measurement rate is of particular interest because entanglement constitutes an important resource for quantum computation. However, to achieve a quantum advantage over classical computation not only entanglement but also so–called *non–stabilizerness*, or *magic*, is a necessary resource. Non–stabilizerness describes the distance between quantum circuits and their closest stabilizer circuits that can be simulated classically with polynomial resources. In this work, we thus pose the question whether there exists a transition of non–stabilizerness in many-body quantum circuits with both measurements and non–stabilizer unitary gates. We numerically compute and analyze the non–stabilizerness of many-body quantum trajectories in such a hybrid quantum circuit employing a recently proposed measure [1, 2].

[1] L. Leone, S.F.E. Oliviero, and A. Hamma, Phys. Rev. Lett. **128**, 050402 (2022).

[2] G. Lami, M. Collura, arXiv:2303.05536 (2023).

## Exponential shortcut to measurement-induced entanglement phase transitions

Ali G. Moghaddam<sup>1,2</sup>, Kim Pöyhönen<sup>2</sup>, Teemu Ojanen<sup>2</sup>

<sup>1</sup> Institute for Advanced Studies in Basic Science (IASBS), Zanjan 45137-66731, Iran

<sup>2</sup> Tampere University, P.O. Box 692, FI-33014 Tampere, Finland

Recently discovered measurement-induced entanglement phase transitions in monitored quantum circuits provide a novel example of far-from-equilibrium quantum criticality. Here, we propose a highly efficient strategy for experimentally accessing these transitions through fluctuations. Instead of directly measuring entanglement entropy, which requires an exponential number of measurements in the subsystem size, our method provides a scalable approach to entanglement transitions in the presence of conserved quantities. In analogy to entanglement entropy and mutual information, we illustrate how bipartite and multipartite fluctuations can both be employed to analyze the measurement-induced criticality. Remarkably, the phase transition can be revealed by measuring fluctuations of only a handful of qubits.

# Temporal Entanglement and Trotter Transitions in unitary quantum circuits

Giuliano Giudici<sup>1</sup>

<sup>1</sup> *Institute for Theoretical Physics, University of Innsbruck, A-6020, Innsbruck, Austria*  
<sup>2</sup> *planqc GmbH, D-85748 Garching, Germany*

It is a notoriously hard problem to access the long-time dynamics of a many-body system after a global quench with tensor network methods, due to the linear growth of entanglement with time. In this talk, I will revisit a clever approach that attempts to overcome this limitation by approximating correlation functions on infinite systems with matrix product states (MPSs) in the temporal direction. I will provide non-trivial examples of strictly discrete dynamics where this MPS approximation becomes efficient (and even exact in some cases!), allowing one to compute expectation values of local observables for arbitrarily long times. Finally, I will discuss how the infinite-time steady state of this discrete dynamics connects to the time-continuum limit, and establish the emergence of sharp transitions as the Trotter step is varied.

- [1] G. Giudice, G. Giudici, M. Sonner, J. Thoenniss, A. Lerose, D. A. Abanin, L. Piroli, *Phys. Rev. Lett.* **128**, 220401 (2022).
- [2] E. Vernier, B. Bertini, G. Giudici, L. Piroli, *Phys. Rev. Lett.* (*Accepted*)

## Computation of Microcanonical Entropy at Fixed Magnetization of the Long-Range Interacting System

Alessandro Campa<sup>1</sup>, Giacomo Gori<sup>2,3</sup>, Vahan Hovhannisyan<sup>4</sup>,  
Stefano Ruffo<sup>5,6</sup> and Andrea Trombettoni<sup>3,5</sup>

<sup>1</sup> *National Center for Radiation Protection and Computational Physics, Istituto  
Superiore di Sanità, Viale Regina Elena 299, 00161 Roma, Italy*

<sup>2</sup> *Dipartimento di Fisica e Astronomia G. Galilei, Università degli studi di Padova,  
via Marzolo 8, 35131 Padova, Italy*

<sup>3</sup> *CNR-IOM DEMOCRITOS Simulation Center, Via Bonomea 265, I-34136 Trieste, Italy*

<sup>4</sup> *A. I. Alikhanyan National Science Laboratory, Alikhanyan Br. 2, 0036 Yerevan, Armenia*

<sup>5</sup> *SISSA, via Bonomea 265, I-34136 Trieste, Italy & INFN, Sezione di Trieste, I-34151  
Trieste, Italy*

<sup>6</sup> *Istituto dei Sistemi Complessi, CNR, via Madonna del Piano 10, I-50019 Sesto  
Fiorentino, Italy*

E-mail: [alessandro.campa@iss.it](mailto:alessandro.campa@iss.it), [gori@sissa.it](mailto:gori@sissa.it), [v.hovhannisyan@yerphi.am](mailto:v.hovhannisyan@yerphi.am), [ruffo@sissa.it](mailto:ruffo@sissa.it),  
[andreatr@sissa.it](mailto:andreatr@sissa.it)

We developed the method to determine the microcanonical entropy at fixed magnetization starting from the canonical partition function. The presented method is based on the introduction of one (or more) auxiliary variables and on a min-max procedure, where the minimization is performed on the variable  $\beta$ , which can be both positive or negative. We emphasized that the method can be very useful where direct counting is not applicable or very difficult/convoluted. We applied our results to the case of systems having long- and short-range (possibly competing) interactions.

**Title- Many-body quantum chaos with randomized measurements**

Authors- Theory: L. Joshi, A. Elben, A. Vikram, B. Vermersch, V. Galitski, P. Zoller

Experiment: K. Collins, A. De, W. Morong, C. R. Monroe

Abstract- The spectral form factor (SFF), characterizing statistics of energy eigenvalues, is a key diagnostic of many-body quantum chaos. In addition, partial spectral form factors (pSFFs) can be defined which refer to subsystems of the many-body system. They provide unique insights into energy eigenstate statistics of many-body systems. We propose a protocol that allows the measurement of the SFF and pSFFs in quantum many-body spin models, within the framework of randomized measurements. Our protocol provides a unified testbed to probe many-body quantum chaotic behavior, thermalization and many-body localization in closed quantum systems. Furthermore, we present implementation of this protocol on a trapped ion quantum simulator employing the use of local random rotations and measurements.

## Scaling Theory of Ergodic Scrambling

**T. Kalsi<sup>1</sup>, A. Romito<sup>1</sup>, and H. Schomerus<sup>1</sup>**

<sup>1</sup>*Department of Physics, Lancaster University, Lancaster LA1 4YB, United Kingdom*

A robust diagnostic tool in the study of late-time quantum chaos is the spectral form factor, calculated from the energy spectrum of a system. While this quantity is well studied for late timescales, a crucial link to most physical settings is its extension to general system dynamics, in particular the approach to ergodicity/chaos, termed 'scrambling'. We investigate the spectral form factor in the context of stochastic quantum dynamics, specifically treating the Wiener process before generalizing to any stochastic process that is invariant under rotations. We aim at a general theory of ergodic/chaotic scrambling which can be turned into a concrete algorithm to analyze any generic system. To this end, we propose a scaling theory that provides a novel route for obtaining a benchmark for dynamics generated from purely stochastic processes, against which we can compare physical systems.

# Simulated cooling of fermionic systems on bosonic quantum hardware

Gilad Kishony<sup>1</sup>, Mark S. Rudner<sup>2</sup>, and Erez Berg<sup>1</sup>

<sup>1</sup>*(Presenting author underlined) Department of Condensed Matter Physics, Weizmann Institute of Science, Rehovot 76100, Israel*

<sup>2</sup>*Department of Physics, University of Washington, Seattle, WA 98195-1560, USA*

We propose an efficient protocol for low energy state preparation of arbitrary gapped fermionic Hamiltonians on a bosonic quantum simulator inspired by the one discussed in [1] for bosonic systems. This procedure involves simulated cooling by coupling the target system with a periodically monitored bath. By fermionizing the simulated target system and the bath, we allow individual fermionic excitations of the system to hop to the bath sites. In this way, we achieve a cooling rate linearly proportional to the density of these excitations, despite the fact that they may be non-local in terms of the bosonic degrees of freedom of the hardware. We apply our protocol to the 1d quantum Ising model which has fermionic excitations, and numerically study its performance in the presence of noise. Our protocol can be applied to any fermionic system, including topological phases in higher dimensions as we discuss in general and apply to the example of the Kitaev honeycomb model. In general, topological states cannot be created from trivial states by finite depth local unitary evolution, which explains the crucial role of measurements used on the monitored bath. States with invertible topological order, such as the chiral p-wave superconductor do not have this limitation, and can be prepared together with their inverse states by such unitaries. This is achieved by our protocol even without the need to monitor the state of the bath after unitary evolution is performed.

[1] A. Matthies, M. Rudner, A. Rosch, E. Berg, arXiv:2210.17256 (2022).

# The Shocks and the Kinks in Josephson Transmission Lines

Eugene Kogan

Bar-Ilan University, Department of Physics

**Contact Information:**

Department of Physics  
Bar-Ilan University  
Ramat-Gan 52900, Israel

Phone: 972-544481223

Email: Eugene.Kogan@biu.ac.il



**Abstract**  
We continue our previous studies of the localized travelling waves, more specifically, of the shocks and the kinks, propagating in the series-connected Josephson transmission line (JTL). The paper consists of two parts. In the first part we calculate the scattering of the "small" (small amplitude small wave vector harmonic wave) on the shock wave. In the second part we study the similarities and the dissimilarities between the shocks and the kinks in the lossy JTL. We also find the particular cases, when the nonlinear equation, describing weak travelling wave in the lossy JTL, can be integrated in terms of elementary functions.

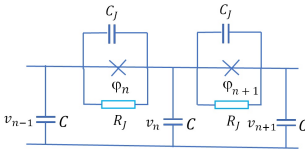


Figure 1: Discrete Josephson transmission line

The circuit equations are

$$h \frac{d\varphi_n}{dt} = v_{n-1} - v_n \quad (1a)$$

$$C \frac{d^2 v_n}{dt^2} = I_c \sin \varphi_n - I_c \sin \varphi_{n+1} + \left( \frac{1}{R_j} + C_j \frac{d}{dt} \right) \frac{h}{2e} (\varphi_n - \varphi_{n+1}), \quad (1b)$$

where  $C$  is the capacitance,  $I_c$  is the critical current of the JJ, and  $C_j$  and  $R_j$  are the capacitor and the ohmic resistor shunting the JJ. In the continuum approximation we treat  $n$  as the continuous variable  $Z$  and approximate the finite differences in the r.h.s. of the equations by the first derivatives with respect to  $Z$ , after which the equations take the form

$$\frac{\partial \varphi}{\partial t} = \frac{\partial V}{\partial Z} \quad (2a)$$

$$\frac{\partial V}{\partial t} = \frac{\partial}{\partial Z} \left( \sin \varphi + \frac{Z_j}{R_j} \frac{\partial \varphi}{\partial t} + \frac{C_j}{C} \frac{\partial^2 \varphi}{\partial t^2} \right), \quad (2b)$$

where we introduced the dimensionless time  $\tau = t/\sqrt{L_j C}$  and the dimensionless voltage  $V = v/(Z_j I_c) \sqrt{L_j} \equiv h/(2eL_j)$  is the "inductance" of the JJ and  $Z_j \equiv \sqrt{L_j/C}$  is the "characteristic impedance" of the JTL.

The sound

$$\frac{\partial \varphi}{\partial \tau} = \frac{\partial V}{\partial Z} \quad (3a)$$

$$\frac{\partial V}{\partial \tau} = -\cos \varphi \frac{\partial \varphi}{\partial Z} \quad (3b)$$

The shocks

$$\bar{U}(\varphi_2 - \varphi_1) = V_1 - V_2, \quad (4a)$$

$$\bar{U}(V_2 - V_1) = \sin \varphi_1 - \sin \varphi_2, \quad (4b)$$

where  $\varphi_1$  and  $V_1$  are the phase and the voltage before the shock,  $\varphi_2$  and  $V_2$  - after the shock, and  $\bar{U}$  is the normalized shock wave velocity. Note also the obvious result of (4a), (4b):

$$\bar{U}^2_{\varphi_2 \varphi_1} = \frac{\sin \varphi_1 - \sin \varphi_2}{\varphi_1 - \varphi_2}, \quad (5)$$

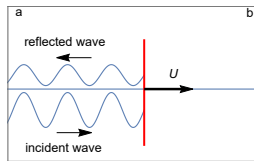


Figure 2: Reflection of a sound wave from a shock wave

$$r \equiv \frac{\varphi(r)}{\varphi(m)} = \frac{[\bar{u}(\varphi_a) - \bar{U}]^2}{[\bar{u}(\varphi_a) + \bar{U}]^2} = \frac{\bar{u}_{in}^2}{\bar{u}_r^2}, \quad (6)$$

where  $\bar{u}_{in} = \bar{u}(\varphi_a) - \bar{U}$  is the velocity of the incident sound wave relative to the shock wave, and  $\bar{u}_r = \bar{u}(\varphi_a) + \bar{U}$  is the velocity of the reflected sound wave relative to the shock wave.

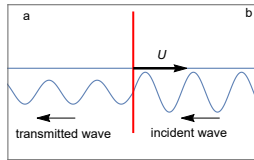


Figure 3: Transmission of a sound wave through a shock wave

$$t \equiv \frac{\varphi(t)}{\varphi(m)} = \frac{[\bar{u}(\varphi_a) + \bar{U}]^2}{[\bar{u}(\varphi_a) - \bar{U}]^2} = \frac{\bar{u}_{in}^2}{\bar{u}_t^2}, \quad (7)$$

where  $\bar{u}_{in} = \bar{u}(\varphi_a) + \bar{U}$  is the velocity of the incident sound wave relative to the shock wave, and  $\bar{u}_t = \bar{u}(\varphi_a) - \bar{U}$  is the velocity of the transmitted sound wave relative to the shock wave.

For the travelling wave we obtain closed equation for  $\varphi$

$$\frac{d^2 \varphi}{d\tilde{\tau}^2} + \gamma \frac{d\varphi}{d\tilde{\tau}} = U^2 \varphi - \sin \varphi + F, \quad (8)$$

where  $\tilde{\tau} \equiv \tau \sqrt{C/C_j} = t/\sqrt{L_j C_j}$ ,  $\gamma \equiv \sqrt{L_j} C_j / R_j$  and  $F$  is the constant of integration.

Localized travelling wave

$$\lim_{\tilde{\tau} \rightarrow -\infty} \varphi = \varphi_1, \quad \lim_{\tilde{\tau} \rightarrow +\infty} \varphi = \varphi_2 \quad (9)$$

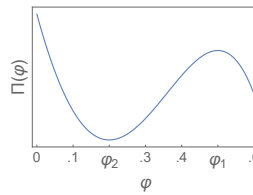


Figure 4: The potential  $\Pi(\varphi)$

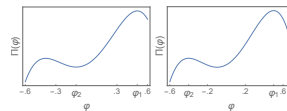


Figure 5: The potential  $\Pi(\varphi)$

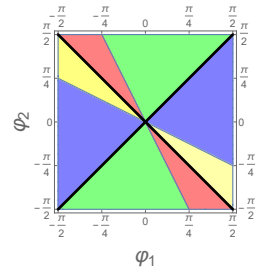


Figure 6: The phase plane of the boundary conditions  $(\varphi_1, \varphi_2)$ . Blue regions correspond to the shock wave moving to the right, green regions - to the left. Yellow regions correspond to the kink moving to the right, red regions - to the left. The thick black line  $\varphi_2 = -\varphi_1$  corresponds to the kink, the thick black line  $\varphi_2 = \varphi_1$  - to the soliton which can exist only in the lossy JTL and propagate in both directions.

**References**

- [1] E. Kogan, Shock wave in series connected Josephson transmission line: Theoretical foundations and effects of resistive elements, Journal of Applied Physics 130, 013903 (2021).
- [2] E. Kogan, The kinks, the solitons and the shocks in series connected discrete Josephson transmission lines, Phys. Stat. Sol. (b) 259, 2200160 (2022).
- [3] E. Kogan, Modulated harmonic wave in series connected discrete Josephson transmission line: the discrete calculus approach, Phys. Stat. Sol. (b) 260, 2200403 (2023).
- [4] E. Kogan, Josephson transmission line revisited, Phys. Stat. Sol. (b) 260, 2200475 (2023).
- [5] E. Kogan, On parametric amplification in Josephson transmission line, Phys. Stat. Sol. (b) 260, 2300005 (2023).
- [6] E. Kogan, On parametric amplification in discrete Josephson transmission line, arXiv:2301.09644v5.
- [7] E. Kogan, The shocks in Josephson transmission line revisited, submitted for publication.

## Theory of free fermion dynamics under partial post-selected monitoring

**C. Leung<sup>1</sup>, D. Meiden<sup>2</sup>, A. Romito<sup>1</sup>**

<sup>1</sup>*Lancaster University, Lancaster, United Kingdom, LA1 4YB*

<sup>2</sup>*Department of Physics, Ben-Gurion University of the Negev, Beer-Sheva 84105, Israel*

Weak continuous measurement is described by the stochastic Schrodinger equation which updates the state according to a random variable associated with the readout. On the other hand, post-selecting all quantum trajectories will lead to a non-Hermitian dynamics. Here, we introduce partial post-selection which interpolates between fully stochastic to non-Hermitian dynamics where some quantum trajectories but not all are kept. We show that the corresponding stochastic Schrodinger equation is modified by a non-Hermitian term which dominates in the limit of strong post-selection. We then investigate the effect it has on measurement induced transition in which it is known that the universality in the fully post-selected limit is different from the fully stochastic limit.

# Abstract: Tunable tachyon mass in the PT-broken massive Thirring model

Benjamin Liégeois

May 2023

We study the full phase diagram of a non-Hermitian PT-symmetric generalization of the paradigmatic two-dimensional massive Thirring model. Employing the non-perturbative functional renormalization group, we find that the model hosts a regime where PT symmetry is spontaneously broken. This new phase is characterized by a relevant imaginary mass, corresponding to monochromatic excitations displaying exponentially growing amplitudes for time-like intervals and tachyonic (Lieb-Robinson-bound breaking, oscillatory) excitations for space-like intervals. Furthermore, since the phase manifests itself as an unconventional attractive spinodal fixed point, which is typically unreachable in finite real-life systems, we find that the effective renormalized mass reached can be tuned through the microscopic parameters of the model. Our results further predict that the new phase is robust to external gauge fields, contrary to the celebrated BKT phase in the PT unbroken sector. The gauge field then provides an effective and easy means to tune the renormalized imaginary mass through a wide range of values, and therefore the amplitude growth/oscillation rate of the corresponding excitations.

## Dynamics of non-gaussianity under continuous measurements

Luca Lumia<sup>1</sup>, Emanuele Tirrito<sup>1,5</sup>, Rosario Fazio<sup>3,4</sup> and Mario Collura<sup>2,3</sup>

<sup>1</sup>*SISSA, Via Bonomea 265, I-34136 Trieste, Italy*

<sup>2</sup>*The Abdus Salam International Centre for Theoretical Physics (ICTP), Strada Costiera 11, 34151 Trieste, Italy*

<sup>3</sup>*INFN Sezione di Trieste, via Bonomea 265, I-34136 Trieste, Italy*

<sup>4</sup>*Dipartimento di Fisica, Università di Napoli “Federico II”, I-80126 Napoli, Italy*

<sup>5</sup>*Pitaevskii BEC Center, CNR-INO and Dipartimento di Fisica, Università di Trento, Via Sommarive 14, Trento, I-38123, Italy*

Measurement induced phase transitions were first described for random circuits, which are prototypical chaotic systems. It was later observed that the entanglement of realistic interacting models has the same phenomenology under continuous measurements: for a small measurement rate below a critical value  $\gamma_c$  the system reaches a volume-law entangled steady state, and for  $\gamma > \gamma_c$  there is a transition towards a Zeno phase, where the entanglement is suppressed. The phase diagram remains the same regardless of the interaction being chaotic or integrable, while free fermions behave differently: the volume law phase is replaced by a logarithmic region. Why such a difference? The most peculiar feature that distinguishes free fermions from other interacting models is gaussianity and we investigate whether non-gaussianity can play a role in determining the entanglement phases of a continuously monitored quantum system.

## On the noisy repeated interaction model

**E. Medina-Guerra<sup>1</sup>, Parveen Kumar<sup>1</sup>, I.V. Gornyi<sup>2</sup>, and Yuval Gefen<sup>1</sup>,**

<sup>1</sup>*Department of Condensed Matter Physics, Weizmann Institute of Science, 760001 Rehovot  
Israel*

<sup>2</sup>*Institute for Quantum Materials and Technologies, Karlsruhe Institute of Technology,  
76021 Karlsruhe, Germany*

A quantum system interacting with a chain of detectors (i.e., auxiliary degrees of freedom) one at a time can be described via a canonical stochastic master equation of the jump type, where the system either evolves continuously in a deterministic and unitary fashion or suffers a discontinuous evolution to a pure state. We generalize this model by introducing an external reservoir that interacts with the chain of detectors and the system and which induces new (and more complicated) terms, both stochastic and deterministic, to the canonical stochastic master equation (**SME**), making it of diffusive-jump type [1]. Contrary to the other canonical stochastic master equation of the diffusive type, the fluctuating generator is unitary and is corrected by an Itô correction in the form of a pure dissipator. The environment also contributes to the deterministic part of the given equation besides the detector's backaction. Moreover, once a jump occurs, it is toward a mixed state, contrasting even more with the canonical jump type equation.

[1] Medina-Guerra, E., Kumar, P., Gornyi, I. V., & Gefen, Y. (2023). Quantum state engineering by steering in the presence of errors. *arXiv preprint arXiv:2303.16329*.

## Distinguishability and complexity in monitored dynamics of bosons

Ken Mochizuki<sup>1,2</sup> and Ryusuke Hamazaki<sup>2,3</sup>

<sup>1</sup>*Department of Applied Physics, University of Tokyo, Tokyo 113-8656, Japan*

<sup>2</sup>*Nonequilibrium Quantum Statistical Mechanics RIKEN Hakubi Research Team, RIKEN Cluster for Pioneering Research (CPR), 2-1 Hirosawa, Wako 351-0198, Japan*

<sup>3</sup>*RIKEN Interdisciplinary Theoretical and Mathematical Sciences Program (iTHEMS), 2-1 Hirosawa, Wako 351-0198, Japan*

Sampling probability distributions of bosons passing through random unitary gates can be hard for classical computers, which can lead to the quantum supremacy [1]. However, sampling bosons in more general dynamics is not always hard and physical situations determine the hardness. From the viewpoint of computational complexity, we explore monitored dynamics of bosons where bosons can be lost into environment but we postselect cases in which all bosons remain in the system. Photons in optical networks experience such non-unitary dynamics, as schematically described in Fig. (a). In particular, we focus on distinguishability of bosons, which is related to the sampling complexity. Indeed, if bosons can be regarded as distinguishable particles, classical computers can sample their probability distribution efficiently.

We show that the bosonic system exhibits a transition related to the distinguishability if the system has Parity and Time-reversal (PT) symmetry [2]. As we increase the strength of loss effect  $\gamma$ , spontaneous breaking of PT symmetry occurs. In the PT symmetric phase, bosons are distinguishable only in the short-time regime due to the absence of quantum interference, which corresponds to the blue region in Fig.(b). On the other hand, in the PT broken phase, bosons become distinguishable not only in the short-time regime but also in the long-time regime, where the latter corresponds to the green region in Fig. (b). In addition, the region where

bosons are distinguishable with small  $t$  is enlarged by the PT symmetry breaking. This distinguishability transition is similar to transitions of entanglement from the volume-law phase to the area-law phase in monitored quantum circuits [3], where classical algorithms based on matrix product states can easily simulate dynamics in the area-law phase. In parallel, sampling the distribution of bosons is classically easy in the PT broken phase, regarding our bosonic system.

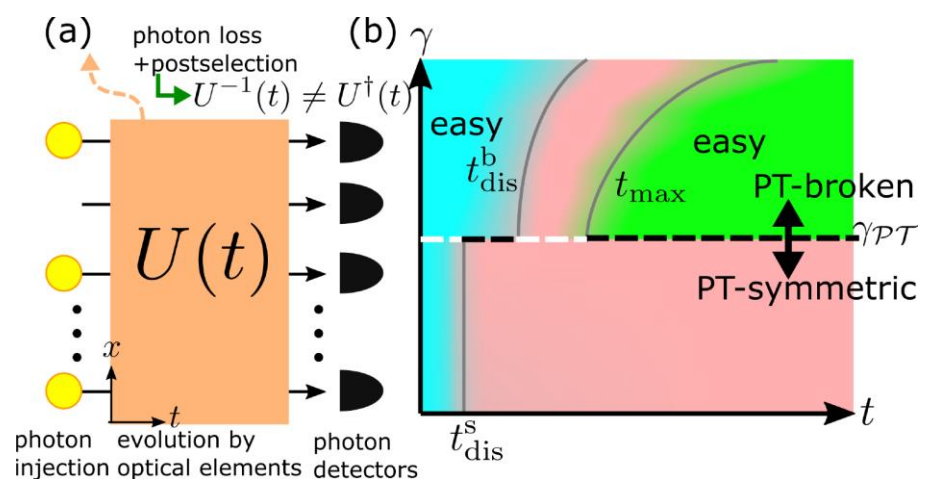


Figure. (a) Schematic picture for non-unitary dynamics of photons in optical networks. (b) Schematic phase diagram of the distinguishability transition in the PT symmetric system.

[1] S. Aaronson and A. Arkhipov, *Theory of Computing* **9**, 143 (2013).

[2] K. Mochizuki and R. Hamazaki, *Phys. Rev. Res.* **5**, 013177 (2023).

[3] B. Skinner, J. Ruhman, and A. Nahum, *Phys. Rev. X* **9**, 031009 (2019).

## Entanglement Transitions in Unitary Circuit Games

**Raúl Morral-Yepes<sup>1,2</sup>, Adam Smith<sup>3,4</sup>, S. L. Sondhi<sup>5</sup>, and Frank Pollmann<sup>1,2</sup>**

<sup>1</sup>*Technical University of Munich, TUM School of Natural Sciences, Physics Department, Lichtenbergstr. 4, 85748 Garching, Germany*

<sup>2</sup>*Munich Center for Quantum Science and Technology (MCQST), Schellingstr. 4, 80799 München, Germany*

<sup>3</sup>*School of Physics and Astronomy, University of Nottingham, Nottingham, NG7 2RD, UK*

<sup>4</sup>*Centre for the Mathematics and Theoretical Physics of Quantum Non-Equilibrium Systems, University of Nottingham, Nottingham, NG7 2RD, UK*

<sup>5</sup>*Rudolf Peierls Centre for Theoretical Physics, University of Oxford, Oxford, UK*

Repeated projective measurements in unitary circuits can lead to an entanglement phase transition as the measurement rate is tuned. In this work, we consider a different setting in which the projective measurements are replaced by dynamically chosen unitary gates that minimize the entanglement. This can be seen as a one-dimensional unitary circuit game in which two players get to place unitary gates on randomly assigned bonds at different rates: The “entangler” applies a random local unitary gate with the aim of generating extensive (volume law) entanglement. The “disentangler”, based on limited knowledge about the state, chooses a unitary gate to reduce the entanglement entropy on the assigned bond with the goal of limiting to only finite (area law) entanglement. In order to elucidate the resulting entanglement dynamics, we consider three different scenarios: (i) a classical discrete height model, (ii) a Clifford circuit, and (iii) a general  $U(4)$  unitary circuit. We find that both the classical and Clifford circuit models exhibit phase transitions as a function of the rate that the disentangler places a gate, which have similar properties that can be understood through a connection to the stochastic Fredkin chain. In contrast, the entangler always wins when using Haar random unitary gates and we observe extensive, volume law entanglement for all non-zero rates of entangling.

[1] R. Morral-Yepes, A. Smith, S. L. Sondhi, and F. Pollmann, Entanglement Transitions in Unitary Circuit Games (2023), arXiv:2304.12965.

# Dynamical Quantum State Reduction models via Spontaneous Unitarity Violation

Spontaneous unitarity violations, a form of spontaneous symmetry breaking, were recently proposed as a cause of objective quantum state reduction. In this poster, we formalise the description of unitarity violations, and show that they generically imply models of dynamical quantum state reduction (DQSR) driven by colored noise. We present a formalism for exploring such models as well as a prescription for enforcing explicit norm-preservation, and we show that the resulting pure state dynamics is described by a modified von-Neumann Liouville equation which in a particular limit reduces to the Gorini-Kossakowski-Sudarshan-Lindblad (GKSL) master equations. We additionally show adherence to Born's rule emerging in the same limit from a physical constraint relating fluctuating and dissipating components of the model. Connections between various topics such as non-equilibrium physics, competition between Unitary evolution and Born's projection are drawn and discussed.

Aritro Mukherjee

PhD candidate

University of Amsterdam

2/08/23

# Measurement-induced criticality in a monitored circuit with U(1) charge conservation

Hisanori Oshima<sup>1</sup>, and Yohei Fuji<sup>1</sup>

<sup>1</sup>(Presenting author underlined) Department of Applied Physics, University of Tokyo, Tokyo 113-8656, Japan

The entanglement entropy shows a phase transition from a volume-law phase to an area-law phase, called measurement-induced entanglement transition, when a pure quantum state evolved under unitary dynamics is subject to local projective measurements. It is intensively studied due to emergence of conformal invariance at the phase transition, which is rarely found in non-equilibrium systems. In this talk, I will discuss critical phenomena in unitary-projective hybrid quantum circuits with U(1) symmetry (charge conservation)[1]. Numerical results show that, in addition to the conventional entanglement transition, a new transition obeying the Tomonaga-Luttinger liquid theory appears. The latter transition is characterized by critical behaviors in steady-state values of a subsystem charge fluctuation[2], a charge correlator, and the entanglement resolved by conserved charges[3]. I also show that a correlator of subsystem charges can be used to locate this new transition point.

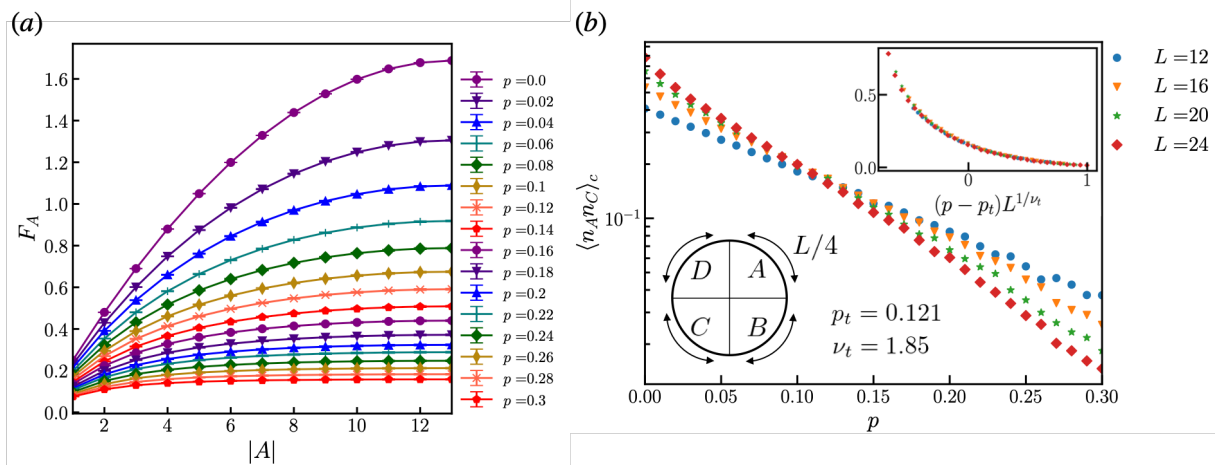


Figure 1: (a) Steady-state value of the bipartite charge-fluctuation  $F_A$  as a function of the subsystem size  $|A|$  for measurement probabilities  $p \in [0.0, 0.3]$ . (b) Steady-state value of the subsystem-charge correlation function  $\langle n_A n_C \rangle_c$  as a function of  $p$ . The inset shows scaling collapse of it.

[1] H. Oshima, Y. Fuji, Phys. Rev. B. **107**, 014308 (2023).

[2] H. Francis Song, *et. al.*, Phys. Rev. B. **85**, 035409 (2012).

[3] J. C. Xavier, F. C. Alcaraz, and G. Sierra, Phys. Rev. B. **98**, 041106 (2018).

## Symmetry-protected topological order and cluster states in open quantum systems

Dawid Paszko, Dominic C. Rose, Marzena Szymańska, Arijeet Pal

*(Presenting author underlined) Department of Physics and Astronomy, University College London, Gower Street, London WC1E 6BT, United Kingdom*

Topological order offers possibilities for storing and manipulating quantum information. Its behaviour in out-of-equilibrium settings has recently become of particular interest because, although susceptible to destroy any order, these are of high experimental relevance. In this work, we demonstrate the ramifications of weak and strong symmetries [1] on the symmetry-protected topological (SPT) phases in open systems. The general principles are illustrated concretely with the archetypal one-dimensional cluster model [2], initially introduced as a platform for measurement-based quantum computation [3].

First, working with the Lindblad master equation [4, 5], we show that the model displays, as a consequence of strong symmetries, two many-body logical qubits in its steady state, characterized by a finite dissipative gap in the thermodynamic limit and metastable under a class of perturbations. We relate these latter properties to the fragmentation of the state space of the problem due to weak symmetries. Second, we also explore the effects of weak symmetries on the dynamics of the model, which are visible in quantum trajectories [6]. We thus find a broad class of dissipation channels that preserve the cluster nature of the states, and hence their SPT features. As a consequence, we show how to recover information stored in edge modes by monitoring quantum jumps in only a small part of the spin chain.

This work thus proposes a new framework to study the effect of symmetries on SPT phases in open quantum systems, and using concrete examples, proves it to be useful whether to engineer dissipation for desired properties or to study their robustness against generic sources of decoherence.

- [1] V. V. Albert, L. Jiang, Phys. Rev. A **89**, 022118 (2014).
- [2] F. Pollmann, A. M. Turner, E. Berg, M. Oshikawa, Phys. Rev. B **81**, 064439 (2010).
- [3] R. Raussendorf and D. E. Browne, H. J. Briegel, Phys. Rev. A **68**, 022312 (2003).
- [4] V. Gorini, A. Kossakowski, E. C. G. Sudarshan, J. Math. Phys. **17**, 821 (1976).
- [5] G. Lindblad, Communications in Mathematical Physics **48**, 119 (1976).
- [6] A. J. Daley, Advances in Physics **63**, 77 (2014).

# Multipartite Entanglement in the Measurement-Induced Phase Transition of the Quantum Ising Chain

Alessio Paviglianiti and Alessandro Silva

*International School for Advanced Studies (SISSA), via Bonomea 265, 34136 Trieste, Italy*

External monitoring of quantum many-body systems can give rise to a measurement-induced phase transition characterized by a change in behavior of the entanglement entropy from an area law to an unbounded growth. We show that this transition extends beyond bipartite correlations to multipartite entanglement. Using the quantum Fisher information, we investigate the entanglement dynamics of a continuously monitored quantum Ising chain. Multipartite entanglement exhibits the same phase boundaries observed for the entropy in the post-selected no-click trajectory. Instead, quantum jumps give rise to a more complex behavior that still features the transition, but adds the possibility of having a third phase with logarithmic entropy but bounded multipartiteness.

## Stability of Nishimori cat states and non-equilibrium entanglement transitions

Malte Pütz, Guo-Yi Zhu, and Simon Trebst

*(Presenting author underlined) Institute for Theoretical Physics, University of Cologne, Zùlpicher Straße 77, 50937 Cologne, Germany*

Shallow quantum circuits that combine unitary gates with non-unitary measurements, so-called monitored quantum circuits, can create long-range entanglement (LRE) in  $O(1)$  steps — substantially faster than local unitary circuits, where entanglement creation is bounded by an information lightcone (Lieb-Robinson bounds). An open question is the stability of such engineered LRE when the circuit itself exhibits imperfections (such as incomplete gate operations or shifted measurements). Here we build on recent work from our group discuss the preparation of “Nishimori cat” states [1], which exhibit a robustness to such imperfections, and explore extensions to imperfect lattice geometries (interpolating between one and two spatial dimensions) and Gaussian coherent noise. We characterize the post-measurement quantum wavefunction by various entanglement quantities and show exotic quantum criticality induced by the inclusion of such circuit imperfections. Our work employs state-of-the-art numerical simulation techniques, including hybrid Monte Carlo / tensor network calculations.

- [1] Guo-Yi Zhu, Nathanan Tantivasadakarn, Ashvin Vishwanath, Simon Trebst and Ruben Verresen, arXiv:2208.11136.

## Abstract for a workshop on Dynamics of Monitored Quantum Many-Body Systems — (smr 3868)

Ritu Nehra<sup>1</sup>, Alessandro Romito<sup>2</sup>, and Dganit Meidan<sup>1</sup>

<sup>1</sup>*Department of Physics, Ben Gurion University of the Negev, Beer-Sheva 84105, Israel*

<sup>2</sup>*Department of Physics, Lanchaster University, Lancaster LA1 4YB, United Kingdom*

The dynamics of entanglement under measurement in many-body quantum systems is a topic under intensive study recently. The generic unitary dynamics give rise to the thermalization in the system due to a highly entangled state, whereas continuous monitoring of these states tends to destroy all the entanglements. The two competing dynamics are responsible for the exciting phase transitions in the quantum systems, which are studied with the help of the entanglement entropy scaling [1]. The experimental probing of these measurements is independent of environmental feedback, which restricts its applicability to a few open systems. In order to capture a large class of environments, the measuring device is modeled as a continuous Gaussian probe in recent work [2] which modify the detector state and use it as feedback to the systems. I will discuss the role of the feedback control measurements in the context of topological phase transitions of the free Fermionic chains. I will discuss how the special measurement operations and environment feedback induced the topology in such a simple system and scale with relative measurement strengths.

- [1] Graham Kells, Dganit Meidan and Alessandro Romito, *Topological transitions in weakly monitored free Fermions*, *SciPostPhys.*14.3.031, 2023.
- [2] M. Szyniszewski, A. Romito, and H. Schomerus, *Entanglement transition from variable-strength weak measurements*, *Phys. Rev. B* 100, 064204, 2019.

# Resetting in the quantum dynamics of a particle in a long-ranged tight-binding model and subject to repeated measurements

Sayan Roy<sup>1</sup>, Shamik Gupta<sup>2</sup>, and Giovanna Morigi<sup>1</sup>

<sup>1</sup> *Theoretische Physik, Universität des Saarlandes, D-66123 Saarbrücken, Germany*

<sup>2</sup> *Department of Theoretical Physics, Tata Institute of Fundamental Research, 1 Homi Bhabha Road, Mumbai, 400005, India*

We analyze the dynamics of a quantum particle moving according to a long ranged tight-binding Hamiltonian and which is additionally subject to repeated projective measurements by a detector placed at the target site. We consider the case of measurements being done both at regular and at random time intervals. In this setup, the ballistic propagation of the particle is found to be constrained by the repeated measurement protocol, which yields a detection probability less than 1. The detection probability is obtained analytically by using a perturbation-theory approach in the spirit of [1]. To get advantage of the ballistic propagation, we extend the model of [2] by resetting at a constant rate, and find the optimal resetting rate required to maximize the detection probability. We finally determine the dependence of the detection probability on the range of the interaction.

[1] S. Dhar, S. Dasgupta, A. Dhar, *J. Phys. A Math.* **48**, 115304 (2015).

[2] R. Yin, E. Barkai, *Phys. Rev. Lett.* **130**, 050802 (2023).

## Full counting statistics as probe of measurement-induced transitions in the quantum Ising chain

Alessandro Santini<sup>1</sup>

<sup>1</sup>*SISSA, via Bonomea 265, 34136 Trieste, Italy\**

Non-equilibrium dynamics of many-body quantum systems under the effect of measurement protocols is attracting an increasing amount of attention. It has been recently revealed that measurements may induce different non-equilibrium regimes and an abrupt change in the scaling-law of the bipartite entanglement entropy. However, our understanding of how these regimes appear, how they affect the statistics of local quantities and, finally whether they survive in the thermodynamic limit, is much less established. Here we investigate measurement-induced phase transitions in the Quantum Ising chain coupled to a monitoring environment. In particular we show that local projective measurements induce a quantitative modification of the out-of-equilibrium probability distribution function of the local magnetization. Starting from a GHZ state, the relaxation of the paramagnetic and the ferromagnetic order is analysed. In particular we describe how the probability distribution of the former shows different behaviour in the area-law and volume-law regimes.

---

\* [asantini@sissa.it](mailto:asantini@sissa.it)

# Symmetry-enriched measurement-only quantum circuits on a Kitaev honeycomb lattice

Daniel Simm, Guo-Yi Zhu, and Simon Trebst

*Institute for Theoretical Physics, University of Cologne, Zùlpicher StraÙe 77, 50937 Cologne, Germany*

Quantum circuits offer unprecedented dynamical control of many-body entanglement, attracting significant attention from quantum information theorists and many-body physicists alike. Even in circuits that are built exclusively from measurements, long-range entanglement can be created through the competition of different, non-commuting measurement operators as shown in a wide variety of models. Previous work, however, primarily focused on measurement-only circuit dynamics with little to no structure. Here we investigate such symmetry-enriched quantum circuits derived from the Kitaev honeycomb model [1, 2, 3] with distinct structures in space and time and characterize the emerging, dynamically created quantum states by their entanglement structure. In doing so, we also study the analytical tractability of random Clifford circuits and discuss a possible computational complexity transition.

- [1] Lavasani et al., arXiv:2207.02877 (2022).
- [2] Sriram et al., arXiv:2207.07096 (2022).
- [3] Zhu et al., arXiv:2303.17627 (2023).

# Entanglement dynamics of free fermions subjected to monitored loss and gain

Elias Starchl<sup>1</sup> and Lukas M. Sieberer<sup>1</sup>

<sup>1</sup> *Institute for Theoretical Physics, University of Innsbruck*

Continuous or repeated projective measurements of site occupation numbers can strongly suppress the creation of entanglement through the unitary dynamics of free fermions hopping along a one-dimensional lattice. This behavior can be understood intuitively in the limit of high measurement rates, where each quantum trajectory, describing the dynamics of the system conditional on a sequence of measurement results, is frozen in a disentangled product state of occupied and empty sites due to the quantum Zeno effect [1]. However, by studying the entanglement dynamics of free fermions subjected to monitored loss and gain, we show that such a freezing of the dynamics is not required to induce a reduction from volume-law to area-law entanglement. Instead, an area-law phase can also emerge from increasingly fast fluctuations of local occupation numbers. Interestingly, while the dynamics induced by measurements of local occupation numbers and monitored loss and gain are strikingly different, we find that in both cases static measures of entanglement indicate a Kosterlitz-Thouless transition between a critical and an area-law phase. Our results shed light on the role of particle number conservation for the occurrence of entanglement transitions in free fermionic systems.

[1] O. Alberton, M. Buchhold, and S. Diehl, *Phys. Rev. Lett.* **126**, 170602 (2021).

## Diagrammatic method for many-body non-Markovian dynamics: memory effects and entanglement transitions

Giuliano Chiriacò<sup>1,2,3</sup>, Mikheil Tsitsishvili<sup>2,3</sup>, Dario Poletti<sup>4,5,2,6</sup>, Rosario Fazio<sup>2,7</sup>, and Marcello Dalmonte<sup>2,3</sup>

<sup>1</sup> *Dipartimento di Fisica e Astronomia “Ettore Majorana”, Università di Catania, 95123 Catania, Italy*

<sup>2</sup> *The Abdus Salam International Centre for Theoretical Physics (ICTP), Strada Costiera 11, 34151 Trieste, Italy*

<sup>3</sup> *SISSA — International School of Advanced Studies, via Bonomea 265, 34136 Trieste, Italy*

<sup>4</sup> *Science, Mathematics and Technology Cluster, Singapore University of Technology and Design, 8 Somapah Road, 487372 Singapore*

<sup>5</sup> *Engineering Product Development Pillar, Singapore University of Technology and Design, 8 Somapah Road, 487372 Singapore*

<sup>6</sup> *Centre for Quantum Technologies, National University of Singapore 117543, Singapore*

<sup>6</sup> *Dipartimento di Fisica, Università di Napoli “Federico II”, Monte S. Angelo, I-80126 Napoli, Italy*

We study the quantum dynamics of a many-body system subject to coherent evolution and coupled to a non-Markovian bath. We propose a technique to unravel the non-Markovian dynamics in terms of quantum jumps, a connection that was so far only understood for single-body systems. We develop a systematic method to calculate the probability of a quantum trajectory, and formulate it in a diagrammatic structure. We find that non-Markovianity renormalizes the probability of realizing a quantum trajectory, and that memory effects can be interpreted as a perturbation on top of the Markovian dynamics. We show that the diagrammatic structure is akin to that of a Dyson equation, and that the probability of the trajectories can be calculated analytically. We then apply our results to study the measurement-induced entanglement transition in random unitary circuits. We find that non-Markovianity does not significantly shift the transition, but stabilizes the volume law phase of the entanglement by shielding it from transient strong dissipation.

[1] Giuliano Chiriacò and Mikheil Tsitsishvili and Dario Poletti and Rosario Fazio and Marcello Dalmonte, arxiv: 2302.10563 (2023).

## Abstract preparation for a Workshop

Caterina Zerba<sup>1,2,3,4</sup>, Alessandro Silva<sup>1,2</sup>

1 International School for Advanced Studies (SISSA), via Bonomea 265,  
34136 Trieste, Italy

2 Università degli Studi di Trieste, via Alfonso Valerio 2, 34127 Trieste, Italy.

3 Department of Physics, Technical University of Munich, 85748 Garching,  
Germany

4 Munich Center for Quantum Science and Technology (MCQST),  
Schellingstr. 4, 80799 München, Germany

We study dynamical phase transitions occurring in the stationary state of the dynamics of integrable many-body non-hermitian Hamiltonians, which can be either realized as a no-click limit of a stochastic Schrödinger equation or using spacetime duality of quantum circuits. In two specific models, the Transverse Field Ising Chain and the Long Range Kitaev Chain, we observe that the entanglement phase transitions occurring in the stationary state have the same nature as that occurring in the vacuum of the non-hermitian Hamiltonian: bounded entanglement entropy when the imaginary part of the quasi-particle spectrum is gapped and a logarithmic growth for gapless imaginary spectrum. This observation suggests the possibility to generalize the area-law theorem to non-Hermitian Hamiltonians.

[1] C. Zerba, A. Silva, arXiv:2301.07383

# Non-Hermitian Generalization of Rényi Entropy in Monitored Quantum Systems

Chao Zheng

*Department of Physics, College of Science, North China University of Technology*

Different concepts and definitions of entropy take key roles in a variety of areas, which can be applied to both classical and quantum systems. Among them is the Rényi entropy, and it is able to characterize various properties of classical information with a unified concise form. However, the conventional Rényi entropy can directly be applied to Hermitian systems only because of the requirement of normalized density matrices. For a non-Hermitian system, the evolved density matrix may not be normalized, the conventional Rényi entropy is not well-defined for non-Hermitian system, including monitored quantum systems [1, 2, 3]. In this talk, we will introduce our recent work [4] that how to describe the Rényi entropy for non-Hermitian systems more appropriately. We obtain a concisely and generalized form of  $\alpha$ -Rényi entropy, and we extend the order- $\alpha$  from finite positive real numbers to zero and infinity. Our generalized non-Hermitian  $\alpha$ -Rényi entropy can be directly calculated using both of the normalized and non-normalized density matrices. We look forward to the applications of our generalized Rényi entropy to describe entropy dynamics of monitored quantum systems.

- [1] Y. Li, X. Chen, Matthew P. A. Fisher, Phys. Rev. B **98**, 205136 (2018).
- [2] B. Skinner, J. Ruhman, A. Nahum, Physical Review X **9**, 031009 (2019).
- [3] Beni Yoshida, arXiv:2109.08691 [quant-ph] (2021).
- [4] D. Li, Chao Zheng, Entropy **24**, 1563 (2022).